MEE08:41

Closed loop power control for LTE uplink

Bilal Muhammad

This thesis is presented as part of Degree of
Master of Science in Electrical Engineering with emphasis on Telecommunications

Blekinge Institute of Technology
School of Engineering

November 2008

Blekinge Institute of Technology
School of Engineering
Department of Signal Processing
Supervisor: Abbas Mohammad
Examiner: Abbas Mohammad

Wireless Access Networks
Ericsson research, Sweden
Supervisor: Per Burström

Abstract

This thesis study involves designing, implementing and testing of a novel radio resource control algorithm for the closed loop power control in the LTE uplink. Different values of the path loss compensation factor are investigated in the range 0.7-1.0 and an optimal value of 0.8 as allowed by the LTE standard is proposed. Both the ideal and a more realistic case modeled by including delay, error, and power headroom reporting were studied.

Simulation results indicated that the closed loop power control with fractional path loss compensation factor is advantageous compared to closed loop power control with full path loss compensation.

Using a simple upload traffic model, the closed loop power control with fractional path loss compensation factor improved the system performance in terms of mean bit rate by 68% in the ideal case and 63% in the realistic case.

The power headroom report triggering at change in path loss gave better performance than triggering at periodic intervals.

Preface

This document summarizes the work carried out at Ericsson research at Lulea, Sweden, as Master Thesis by Bilal Muhammad, Electrical Engineering student from the Blekinge Tekniska Högskola (BTH).

Acknowledgment

I would like to acknowledge and extend my heartfelt gratitude, to my thesis supervisor **Per Burström** at Ericsson research Lulea, for his support and encouragement which has made the completion of this thesis possible. Throughout my work with this thesis, I have received so much help from him. Thanks for catching my misunderstandings and unclear wordings and thereby greatly improving the quality of this report. Thanks also for all his ideas and suggestions; they have guided me to improve my technical and non-technical skills as well. This thesis would have been an uninspired struggling little piece of work without your help.

Special thanks to **Arne Simonsson** for answering my questions and helping me to understand the simulation results and commenting on them. His support and guidance helped me to understand my thesis work in a better way. He always showed me a way whenever I found it hard to understand things. I would also like to thank **Magnus Thurfjell** for his time and support.

My greatest appreciation also goes, to my supervisor **Abbas Mohammad** at Blekinge Tekniska Högskola (BTH), for his advice, time and interest**.**

Finally, I thank my friends and family for supporting me throughout all my studies at BTH. Their love and affection didn't make me feel that I am alone.

Karlskrona, 5th of Nov 2008

_____

Bilal Muhammad

Table of Contents

List of Figures

Acronyms and Notations

Acronyms

Acronym	Description
3GPP	Third Generation Partnership Project
ARQ	Automatic repeat request
CDF	Cumulative distribution function
CDMA	Code division multiple access
DL	Downlink
eNB	Evolved Node-B
FDD	Frequency division duplex
FDMA	Frequency division multiple access
FDMA	Frequency division multiple access
HARQ	Hybrid ARQ
LOS	Line of sight
LTE	Long-Term Evolution
MIMO	Multiple input, multiple output
OFDM	Orthogonal frequency division multiplexing
OFDMA	Orthogonal frequency division multiple access
PAPR	Peak-to-average power ratio
PHY	Physical layer
PL	Path loss
PRB	Physical Resource block
PSD	Power spectral density
PUSCH	Physical uplink shared channel
QAM	Quadrature amplitude modulation
QPSK	Quadrature phase shift keying
RRC	Radio resource control
RRM	Radio resource management
RSRP	Reference signal received power
RTT	Round trip time
SDMA	Spatial-Division Medium Access
SINR	Signal-to-interference-and-noise ratio
SNR	Signal-to-noise ratio
TDD	Time division duplex
TDM	Time division multiplexing
TDMA	Time division multiple access
TPC	Transmit power control
TTI	Transmission time interval
UE	User equipment
UL	Uplink
UTRA	Universal terrestrial radio access
UTRAN	Universal terrestrial radio access network

Notation

μ	Filter parameter
γ	Path loss exponent
δ_{mcs}	LTE modulation and coding scheme
$abserr$	Absolute error
B	Transmission bandwidth
g	Gain
l	Loss
M	Number of physical resource blocks
N_0	Noise power spectral density
P_I	Interference power
PL	Path loss
PL_{max}	Maximum path loss
P_{max}	Maximum allowed power
P_n	Noise power
P_{OL}	UE uplink power set by open loop power control
P_{PUSCH}	UE power in the PUSCH
P_{rx}	Received power
P_{tx}	Transmitted power
SNR_0	Open loop SNR target
α	Path loss compensation factor
β	Constant specific to antenna parameter
Δ_i	Closed loop correction value

Chapter 1 Introduction

This chapter includes the thesis introduction, including scope and thesis objective. To facilitate the reader, thesis outlines are also added.

1.1 Thesis objective

The objective of this thesis study is to design and implement the closed loop power control scheme in combination with the fractional path loss compensation factor for the physical uplink shared channel (PUSCH). Furthermore, to investigate different values for the path loss compensation factor and choose an optimal value that results in best cell edge and mean user throughput.

1.2 Thesis scope

The scope of the thesis is limited to the closed loop power control for the PUSCH only. The specifications for the 3GPP Long Term Evolution (LTE) supports advanced antenna systems including multiple transmit and receive antennas i.e. multiple-input and multiple-output (MIMO), but for practical reasons this study is limited to single transmit and receive antenna systems i.e. single-input and single-output (SISO). MIMO systems can achieve better performance, but the aim of this thesis is to provide a relative comparison between methods not to find absolute values on performance.

3GPP LTE can be used in both paired (FDD) and unpaired (TDD) spectrum. This thesis focuses on FDD. LTE is designed to support flexible carrier bandwidths from below 5MHz up to 20MHz, in many spectrum bands. This study only deals with 10MHz bandwidth. The scheduling algorithm used by eNB is pure time division multiplexing (TDM).

1.3 Assessment methodology

The implementation and simulations are carried out using a multi-cell radio network dynamic simulator implemented in MATLAB. The simulator includes enhanced traffic and Hybrid ARQ (HARQ) models. In the simulator, the network performance is simulated for a certain period of time, which then includes events like arrival of new users, departure of users (whose calls are finished) and user movement. The simulator also includes a set of radio resource management (RRM) algorithms such as cell selection, scheduling, link adaptation, and transmit beam forming. A detailed explanation of the simulation environment is presented in Appendix A.

In order to evaluate the performance in terms of system, as well as user performance of different power control schemes and the implemented closed loop algorithm, a set of key performance indicators (KPIs) have been chosen.

Cell-edge user throughput: The cell edge user throughput is defined as the 5^{th} percentile point of the Cumulative Distribution Function (CDF) of user throughput. It is an indicator of the coverage performance.

Average per-user throughput: The average per-user data throughput is defined as the sum of the average data throughput of each user in the system divided by the total number of users in the system. The average per-user throughput is also referred to as average or mean user throughput.

Uplink received signal-to-interference and noise ratio (SINR): CDF plot of user SINR distribution in the uplink, representing both 5^{th} percentile and mean per-user SINR.

Power utilization: CDF plot of power utilization. It provides the percentage of users using maximum allowed power for communication.

1.4 Thesis outlines

Chapter 2 provides the theoretical background about wireless communication channel impairments and fundamentals of cellular networks. It also presents an overview of the capabilities of the long term evolution (LTE) and the physical layer of the LTE. The theoretical background about power control schemes and PUSCH power control formula is also included in this chapter. Furthermore, with the help of mathematical expressions and figures, the underlying differences between power control schemes are also explained.

Chapter 3 describes the problem statement and a mathematical representation of the implemented solution. It also describes implementation methodology and issues involved in the implementation. The methodology includes implementation of closed loop with full path loss compensation, closed loop with fractional path loss compensation factor and SINR filtering. Moreover, the text also explains absolute error and delay models and its implementation.

Simulation results and analysis are presented in Chapter 4. The conclusions can be found in Chapter 5, followed by the discussion of possible continuation of this thesis work.

Chapter 2 Background

This chapter provides the user a preliminary background about the channel impairments in wireless communication and fundamentals of cellular network. This chapter also includes a short overview of Long Term Evolution (LTE) and its key features, followed by a brief introduction of the physical layer (PHY) of LTE .It also provides the reader with motivations for the relevance of the power control problem. Furthermore, this chapter describes LTE PUSCH power control and also explains different power control algorithms.

2.1 Wireless communication system

The main difference between a wireless communication system and a wireline system is the channel. A wire has stationary characteristics, whereas the wireless channel changes with time since the environment between the transmitter and the receiver changes. It is not only susceptible to noise, interference, and other channel impediments, but these impediments change over time in unpredictable ways due to user movement. This section describes some of the basic channel impairments.

2.1.1 Radio signal propagation

Performance in a wireless system is limited by radio signal propagation. A radio signal is a form of electromagnetic waves and obeys the basic laws that govern this type of waves [17]. As an electromagnetic wave propagates through the air, it is attenuated due to reflection, diffraction, refraction and scattering. This attenuation or loss l is defined as the ratio of transmitted signal power P_{tx} to received signal power P_{rx}.

$$l = \frac{P_{tx}}{P_{rx}} > 1 \tag{2-1}$$

The inverses of loss l is the gain g, defined as

$$g = \frac{P_{rx}}{P_{tx}} < 1 \tag{2-2}$$

The value of g, or equivalently l, depends on the propagation conditions. We are interested in the power of the received signals. In order to model this, the propagation effect is separated in three groups and modeled as

$$g = g_{pathgain} \cdot g_{shadowing} \cdot g_{multipath} \tag{2-3}$$

The distance dependent attenuation is modeled by the path loss ($g_{pathgain}$). The terrain variations are resulting in shielding and diffraction and are modeled by the shadow fading or shadowing ($g_{shadowing}$), while the effects of the reflections are captured by the multipath fading or multipath ($g_{multipath}$). These models are further explored below. For more extensive material regarding radio wave propagation, see [12].

2.1.1.1 Path loss

One of the simplest models is based on the assumption of propagation in free space, but except for satellite communication applications, this is too coarse. When we consider propagation over plane earth an approximation of the signal attenuation caused by the distance travelled is derived in [13], and given by

$$PL = \beta \cdot R^{\gamma} \tag{2-4}$$

or

$$g_{pathgain} = \frac{1}{\beta \cdot R^{\gamma}} \tag{2-5}$$

where R is the distance between the transmitter and the receiver, the path loss exponent γ is a constant equal to 4, and β is a constant which depends on antenna specific parameters and the transmitted wavelength.

Empirical studies by Okumura [14] and Hata [15] resulted in path loss models for urban, suburban and rural areas. Typical values of γ are about 2−5, where the lowest value corresponds to free space propagation, and the higher to urban environments with high buildings.

2.1.1.2 Shadow fading

In addition to path loss due to distance, a transmitted signal will be attenuated by objects blocking the line-of-sight (LOS) path between transmitter and receiver. This attenuation is referred to as shadow fading and is usually modeled as a lognormal distribution.

$$g_{shadowing} \sim N(0, \sigma_s) \tag{2-6}$$

where $g_{shadowing}$ is the shadow fading with zero-mean Gaussian random variable with a variance of σ^2.

2.1.1.3 Multipath fading

Before describing the multipath fading it is essential to explain the phenomenon of reflection, diffraction and scattering as shown in Figure 2-1.

When an object is large compared to the wavelength of the signal e.g. huge buildings, mountains or the surface of the earth, the signal is reflected. The phenomenon of

refraction takes place when the velocity of signal changes due to the change in density of a medium through which it travels. The electromagnetic wave bent towards the medium when it travels into a relatively dense medium. This is the reason for the line of sight (LOS) radio waves bent towards the earth as the density of the atmosphere is higher closer to the ground.

An incoming signal is scattered into several weaker signal when it encounters a surface less than or equal to its wavelength e.g. tree leaves, twigs and tree branches. Diffraction occurs when the radio path between the transmitter and receiver is obstructed by a surface with irregular edges. This gives rise to bending of waves around the obstacle, even when a line-of-sight path does not exist between transmitter and receiver.

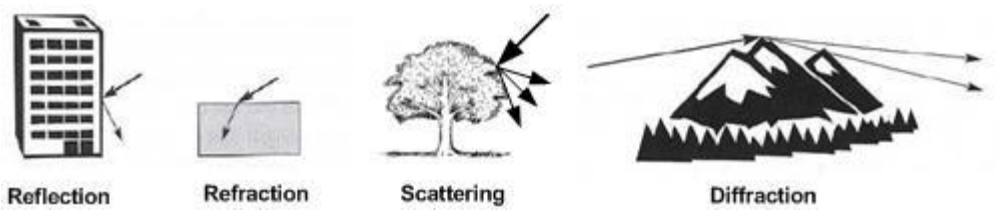

Figure 2-1: Illustration of reflection, refraction, scattering, diffraction of a radio wave

A radio signal transmitted from a fixed source will encounter multiple objects in the environment that produce reflected, diffracted, or scattered copies of the transmitted signal, as shown in Figure 2-1. These additional copies of the transmitted signal, called multipath signal components, can be attenuated in power, delayed in time, and shifted in phase and/or frequency from the LOS signal path at the receiver. The multipath and transmitted signals are summed together at the receiver, which often produces distortion in the received signal relative to the transmitted signal.

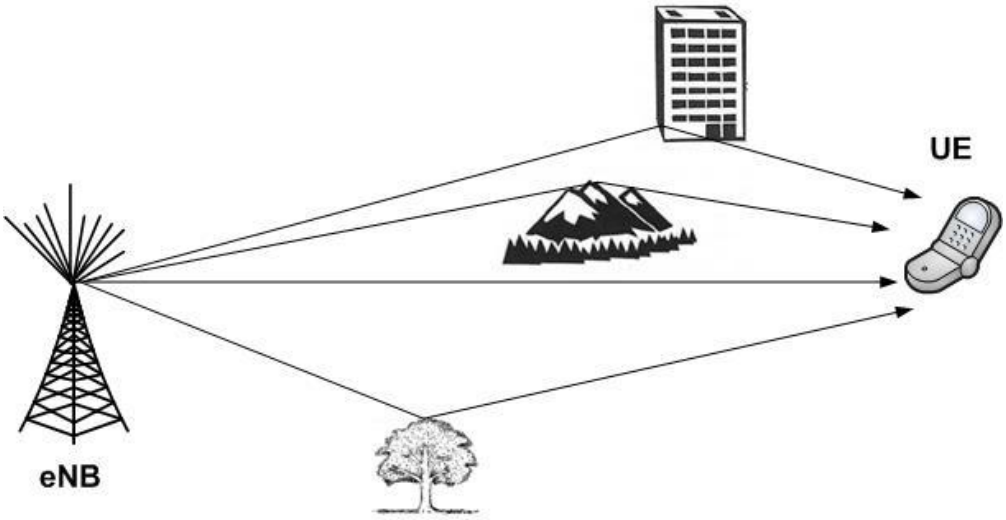

Figure 2-2 : Reflected, diffracted, scattered, and directed wave components

2.1.2 Cellular network fundamentals

The geographic area covered by a cellular network is split into smaller units, where each unit is served by its own base station. These smaller units are called cells in networks with omnidirectional antennas and sectors in networks with directional antennas.

Cell site

A cell site or site is a base station or the geographic location of a base station. The cell site is equipped with transmission and reception equipment, including the base station antenna, which connects an electronic device (cellular phone, laptops etc) to the network.

Base station coverage area

A base station coverage area is the geographic area covered by a base station.

Cell

In networks with omnidirectional antennas, a cell is synonymous with a base station coverage area. In networks with directional antennas, a cell or a sector is the subdivision of a base station coverage area resulting from the use of directional antennas. The Figure 2-3 shows the difference between cell using omnidirectional antenna and cell/sector using directional antenna. In this thesis study, the simulations are carried out using network with directional antenna therefore a cell is referred to as a sector.

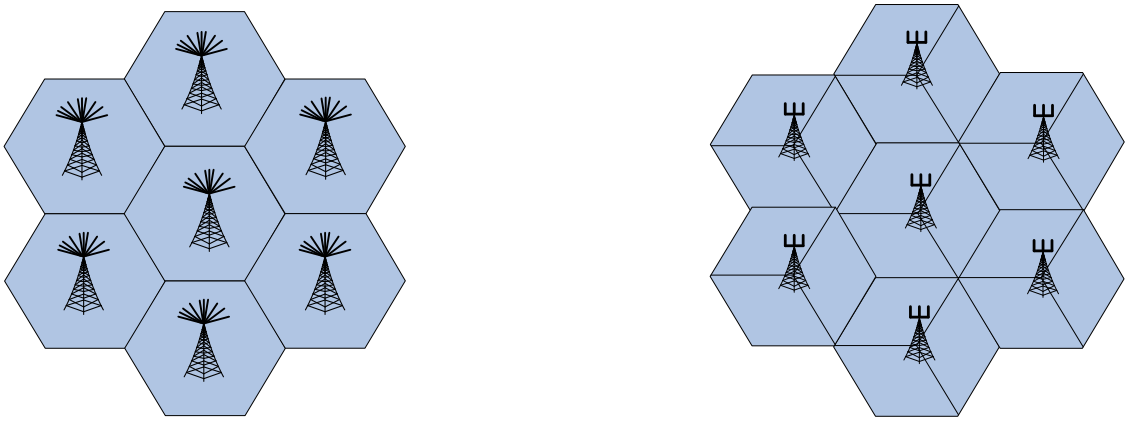

(a) **(b)**

Figure 2-3: (a) Seven cells each using omnidirectional antennas (b) Seven sites each consisting of 120^{o} directional antenna i.e. each with 3-sectors or cells per site.

2.1.2.1 Multiple access techniques

Spectral sharing in communication systems, also called multiple access, is done by dividing the signaling dimensions along the time, frequency, and/or code space axes. In frequency-division multiple access (FDMA), the total system bandwidth is divided into orthogonal frequency channels. In time-division multiple access (TDMA), time is divided orthogonally and each channel occupies the entire frequency band over its assigned timeslot. In orthogonal frequency division multiple access (OFDMA), subcarriers are grouped into larger units, referred to as sub-channels, and these sub-channels are further grouped into bursts which can be allocated to wireless users. Code-division multiple access (CDMA) is typically implemented using direct-sequence or frequency-hopping spread spectrum with either orthogonal or non-orthogonal codes.

The cellular systems using orthogonal multiple access techniques are termed as orthogonal systems and those using non orthogonal multiple access schemes are known as non orthogonal systems.

2.1.2.2 Coverage

Coverage refers to the number of base stations or cell sites that are required to “cover” or provide service to a given area with an acceptable grade of service. This is an important consideration when a cellular system is first deployed. Clearly the cellular system that requires the fewest number of cell sites to cover a given geographic area has an infrastructure cost advantage.

The number of cell sites that are required to cover a given area is determined by the maximum allowable path loss and the path loss characteristic.

2.1.2.3 Capacity

The cell capacity or sector capacity is equal to the number of available voice/data channels per cell or sector.

2.1.2.4 Frequency reuse

The basic premise behind cellular systems is to exploit the power falloff with distance of signal propagation to reuse the same channel at spatially-separated locations. Specifically, the coverage area of a cellular system is divided into non-overlapping cells where some set of frequencies or channels is assigned to each cell. This same channel set is used in another cell some distance away. The reuse of channels is called frequency reuse or channel reuse.

2.1.2.5 Interference

The interference arises when the same carrier frequency is used in different cells is called intercell interference. The cells that are assigned the same channel set are called co-channel cells. The inter-cell interference is also referred to as co-channel interference. It is one of the major factors which limits the capacity of cellular systems.

In addition, systems with non-orthogonal channelization, leads to interference from within a cell, called intracell interference. This intracell interference also arises in systems with orthogonal channelization when multipath, synchronization errors, and other practical impairments compromise the orthogonality. However, orthogonal multiple access techniques have no intracell interference under ideal operating conditions.

2.1.2.6 Signal to noise power ratio

The received signal-to-noise power ratio (SNR) is the ratio of the received signal power P_r to the power of the noise within the bandwidth B of the transmitted signal. The received power is determined by the transmitted power and the path loss, shadowing, and multipath fading. The noise power is determined by the bandwidth of the transmitted signal and the spectral properties of noise.

Since the noise has uniform power spectral density $N_0/2$, the total noise power within the bandwidth $2B$ is $P_{noise} = N_0/2 \times 2B = N_0 B$. So the received SNR is given by

$$SNR = \frac{P_r}{N_0 B} \tag{2-7}$$

In systems with interference, we often use the received signal-to-interference-plus-noise power ratio (SINR) in place of SNR for calculating error probability. The received SINR is given by

$$SINR = \frac{P_r}{N_0 B + P_I} \tag{2-8}$$

where P_I is the average power of interference.

2.2 Long Term Evolution – LTE

3GPP LTE represents a major advance in cellular technology. LTE is designed to meet carrier needs for high-speed data and media transport as well as high-capacity voice support. It provides high-speed data; multimedia unicast and multimedia broadcast services. LTE offers several important benefits which are listed below.

Capacity and performance

LTE provides downlink peak rates of at least 300Mbps and uplink peak rates of 50Mbps in 20 MHz channel. LTE leverages advanced antenna techniques such as MIMO, SDMA and beamforming, which provides benefits to users in both high and low signal strength areas.

Simplicity

LTE supports flexible carrier bandwidths; from below 5MHz up to 20MHz. It also supports both FDD (Frequency Division Duplex) and TDD (Time Division Duplex). Its radio network products will have a number of features that simplify the building and management of next-generation networks. For example, features like plug-and-play, self-configuration and self-optimization will simplify and reduce the cost of network roll-out and management. LTE will be deployed in parallel with simplified, IP-based core and transport networks that are easier to build, maintain and introduce services on.

Wide range of terminals

In addition to mobile phones, many computer and consumer electronic devices, such as notebooks, ultra-portables, gaming devices and cameras, will incorporate LTE embedded modules. Since it supports hand-over and roaming to existing mobile networks, all these devices can have ubiquitous mobile broadband coverage from day one.

2.2.1 LTE physical layer

2.2.1.1 Multiplexing Schemes

The capabilities of the evolved node-B (eNB) and the user equipment (UE) are obviously quite different, thus the LTE physical layer (PHY) downlink (DL) and uplink (UL) are different.

Downlink

Orthogonal Frequency Division Multiplexing (OFDM) is selected as the basic modulation scheme because of its robustness in the presence of severe multipath fading. Orthogonal Frequency Division Multiple Access (OFDMA) is employed as the multiplexing scheme in the downlink.

Uplink

LTE uplink requirements differ from downlink in several ways. Power consumption is a key consideration for UE terminals. High peak-to-average power ratio (PAPR) and related loss of efficiency with OFDM signaling are major concerns. As a result, an alternative to OFDMA was sought for use in the LTE uplink.

LTE PHY uses Single Carrier- Frequency Division Multiple Access (SC-FDMA) as the basic transmission scheme for the uplink. SC-FDMA is a modified form of OFDMA. SC-FDMA has similar throughput performance and overall complexity as OFDMA. The principle advantage of SC-FDMA is the lower PAPR than OFDMA.

2.2.1.2 Frame structure

In uplink, LTE transmissions are segmented into frames, where a frame consists of 10 sub-frames and a sub-frame is formed by two slots of duration of 0.5 ms each consists of 7 SC-FDMA symbols.

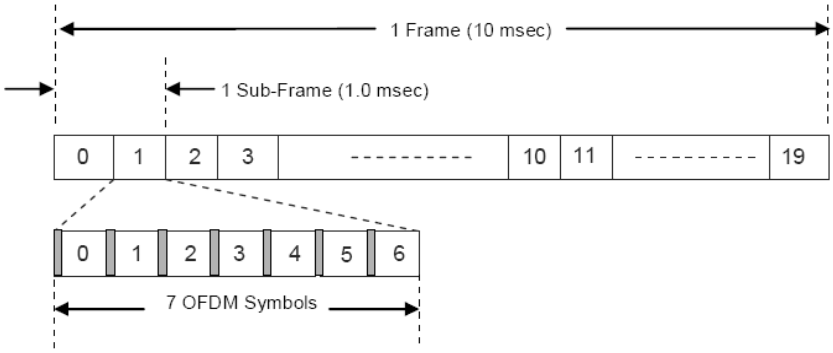

Figure 2-4: LTE generic frame structure

2.2.1.3 Physical resource block

In LTE, physical resource block (PRB) is the smallest element of resource allocation assigned by the base station scheduler. A PRB is defined as a resource of 180 kHz in the frequency domain and 0.5 ms (1 time slot) in time domain. Since the subcarrier spacing is 15 kHz, each PRB consists of 12 subcarriers in frequency domain.

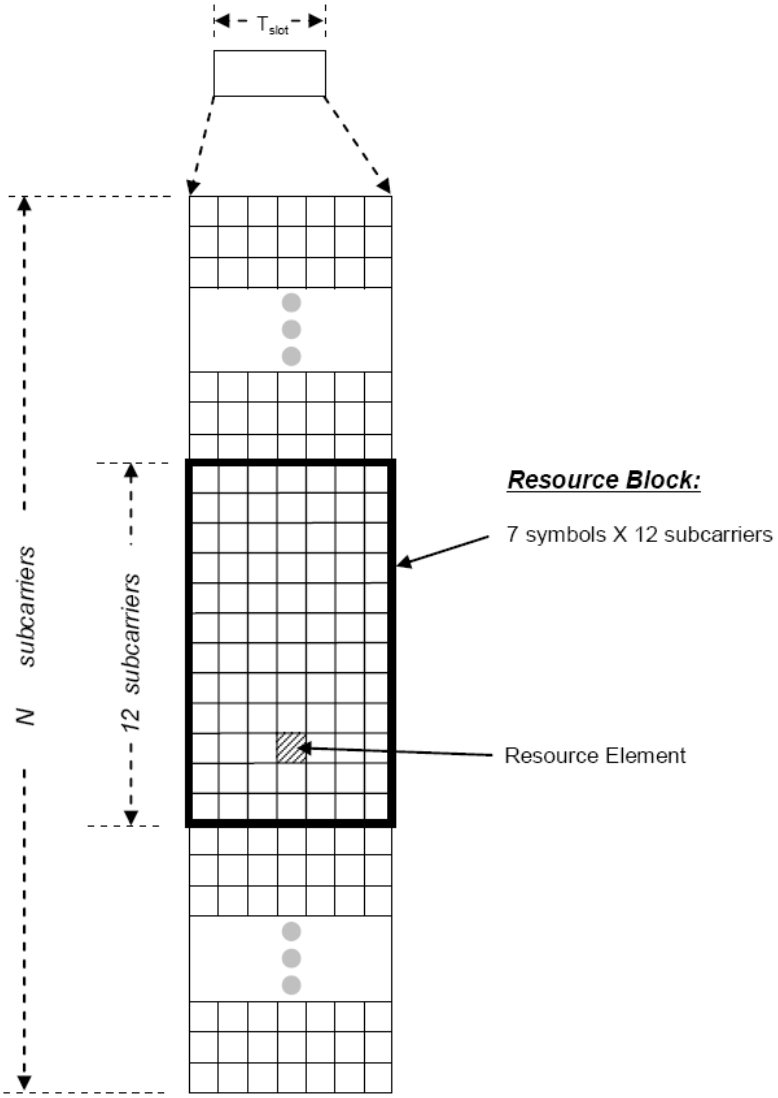

Figure 2-5: LTE uplink resource grid

2.2.1.4 Physical uplink shared channel – PUSCH

PUSCH is used to carry user data. Resources for the PUSCH are allocated on a sub-frame basis by the UL scheduler. Subcarriers are allocated in multiples of 12 (PRBs) and may be hopped from sub-frame to sub-frame. The PUSCH may employ QPSK, 16QAM or 64QAM modulation.

2.2.1.5 Reference Signals

LTE employs special reference signals to facilitate carrier offset estimate, channel estimation, timing synchronization etc. Reference signals are embedded in the PRBs as shown in Figure 2-6.

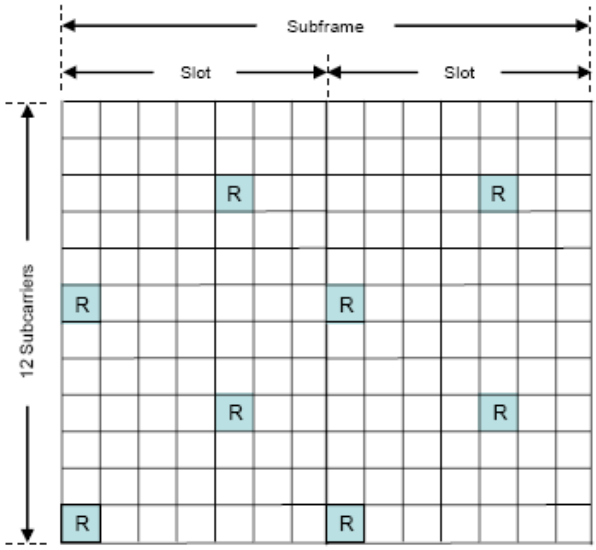

Figure 2-6: Resource element mapping of reference signals for single antenna only

Reference signals are transmitted during the first and fifth OFDM symbols of each time slot and every sixth subcarrier of each sub-frame. Reference signal is also used to estimate the path loss using reference symbol received power (RSRP).

2.3 Role of power control

Better capacity

In a multi user environment a number of user shares the same radio resources. A consequence of the limited availability of radio channels in the network is that the same channel has to be assigned to many users. Thus a signal intended for a certain user will reach other users and introduce interference to their connection, and degrade the quality. A user with very good quality may consider using a low power and still having acceptable quality. The advantage is that it will disturb other users less, and thereby their quality is improved. Power control is essentially to do the same thing but in a controlled manner.

LTE uses SC-FDMA as its radio access technology in the uplink. Usage of an orthogonal transmission scheme eliminates mutual interference between users in the same cell so called intra-cell interference and near-far problem as of typical CDMA systems. But as transmission in the neighboring cell is not orthogonal, so there is interference between users in the neighboring cells that is inter-cell interference, which ultimately limits the system performance in terms of capacity.

To maximize spectral efficiency, 3GPP LTE is designed for frequency reuse 1 [1] both for downlink and uplink, which means that all cells in the network use the same frequency bands. Thus with frequency reuse 1, both data and control channels are sensitive to inter-cell interference. The cell edge performance and the capacity of a cell

site can be limited by the inter-cell interference. Therefore the role of closed loop power control becomes decisive to provide the required SINR to maintain an acceptable level of communication between the eNB and the UE while at the same time controlling interference caused to neighboring cells.

Battery power consumption

Battery power is a scare resource for portable devices like notebooks, ultra-portables, gaming devices and video cameras. In the coming years these devices will operate over mobile broadband technology such as LTE. Therefore to minimize consumption of battery power and use the available power efficiently, power control can be helpful.

2.4 LTE PUSCH power control

Power control refers to set output power levels of transmitters, base stations in the downlink and UEs in the uplink. The 3GPP specifications [1] defines the setting of the UE transmit power for PUSCH by the following equation

$$P_{PUSCH} = \min\{P_{\max}, 10 \cdot \log_{10} M + P_0 + \alpha \cdot PL + \delta_{mcs} + f(\Delta_i)\} \text{ [dBm]} \quad (2\text{-}9)$$

where

- $P_{\max}$ is the maximum allowed transmit power. It depends on the UE power class.
- M is the number of physical resource blocks (PRB).
- P_0 is cell/UE specific parameter signaled by radio resource control (RRC). In this thesis study, it is assumed that P_0 is cell-specific.
- α is the path loss compensation factor. It is a 3-bit cell specific parameter in the range [0 1] signaled by RRC.
- PL is the downlink path loss estimate. It is calculated in the UE based on the reference symbol received power (RSRP).
- δ_{mcs} is cell/UE specific modulation and coding scheme defined in the 3GPP specifications for LTE. However, δ_{mcs} is not included in this thesis study.
- $f(\Delta_i)$ is UE specific. Δ_i is a closed loop correction value and f is a function that permits to use accumulate or absolute correction value.

P_0 is calculated [2] as

$$P_0 = \alpha \cdot (SNR_0 + P_n) + (1-\alpha)(P_{\max} - 10 \cdot \log_{10} M_0) \text{ [dBm]} \quad (2\text{-}10)$$

where

- SNR_0 is the open loop SNR target.
- P_n is the noise power per PRB.
- M_0 defines the number of PRBs for which the SNR target is reached with full power. It is set to 1 in the implementation for simplicity.

2.4.1 PUSCH power control signaling

The parameters involved in eq. (2-9), out of these parameters, few of the parameters are broadcast by the eNB i.e. same for all the users in that specific cell. The figure shown below helps more in understanding the parameters signaled by the eNB towards the UEs.

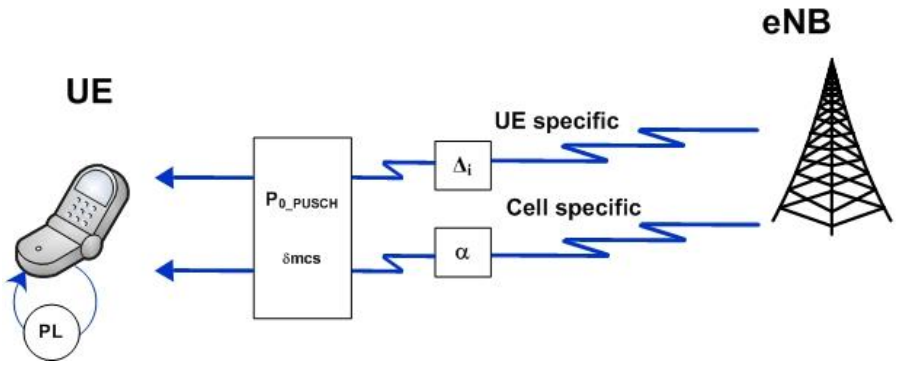

Figure 2-7: PUSCH power control parameters broadcasted by the eNB towards the UEs

Figure 2-7 shows that the UE received parameters namely Δ_i, α, P_0 and δ_{mcs} from the eNB. *PL* is the estimate of the path loss calculated at the UE based on reference symbol received power (RSRP). It is also indicated in figure that few parameters are cell specific i.e. these parameters vary from UE to UE. Cell specific parameters indicate that they are same for all the UEs in that specific cell.

2.4.2 Power spectral density - PSD

UE sets its initial transmission power based on received parameters from the eNB and path loss calculated by the UE. It is worthwhile to note that Δ_i is signaled by the eNB to any UE after it sets its initial transmit power i.e. Δ_i have no contribution in the initial setting of the UE transmit power. The expression, based on which a UE sets its initial power can be obtained from eq. (2-9) by ignoring δ_{mcs} and the closed loop correction while power limitation can be neglected since it corresponds to the UE to respect it.

$$P_{PUSCH} = 10 \cdot \log_{10} M + P_0 + \alpha \cdot PL \ \left[\text{dBm}\right] \tag{2-11}$$

where *M* is the total number of PRB scheduled by the eNB. The power assignment for transmission at the UE is performed on the basis of PRB and each PRB contains equal amount of power. Thus by neglecting *M*, the expression used by the UE to assign power to each PRB is given by

$$PSD_{Tx} = P_0 + \alpha \cdot PL \ \left[\text{dBm / PRB}\right] \tag{2-12}$$

The eq. (2-12) represents transmit power spectral density (PSD) of a PRB expressed in dBm/PRB. PSD_{Tx} is a helpful means to explain the basic difference between conventional and fractional power control. This is discussed in next section.

The power control scheme can be categorized based on the value of α in eq. (2-12).

Figure 2-8: Power control schemes categorized based on the value of α

Using α = 1 (full compensation of path loss) leads to conventional power control. $0 < \alpha < 1$ (fractional compensation of path loss) turns to fractional power control, while α = 0 (no compensation of path loss) leads to no power control i.e. all users will use maximum allowed transmission power.

2.4.3 Conventional power control scheme

Using $\alpha = 1$, P_0 is given below

$$P_0 = SNR_0 + Pn \ \left[\text{dBm}\right]$$

And thus the PSD_{Tx} is given by

$$PSD_{Tx} = P_0 + PL = SNR_0 + Pn + PL \ \left[\text{dBm / PRB}\right] \quad (2\text{-}13)$$

Taking into account the path loss, received PSD at the eNB is given by

$$PSD_{Rx} = (SNR_0 + Pn) = P_0 \ \left[\text{dBm / PRB}\right] \quad (2\text{-}14)$$

It is important to note that the received PSD at the eNB is equal to $P_{0,}$ thus eq. (2-14) illustrates that a conventional PC scheme steers all users with equal power spectral density. This scheme is widely used in cellular systems which are not using orthogonal transmission scheme in the uplink such as CDMA based systems. One of the advantages of this power control scheme is that it removes near-far problem as of typical CDMA systems, since it equalizes power of all UEs before receiving at the base station. The received PSD is plotted for users of different path loss.

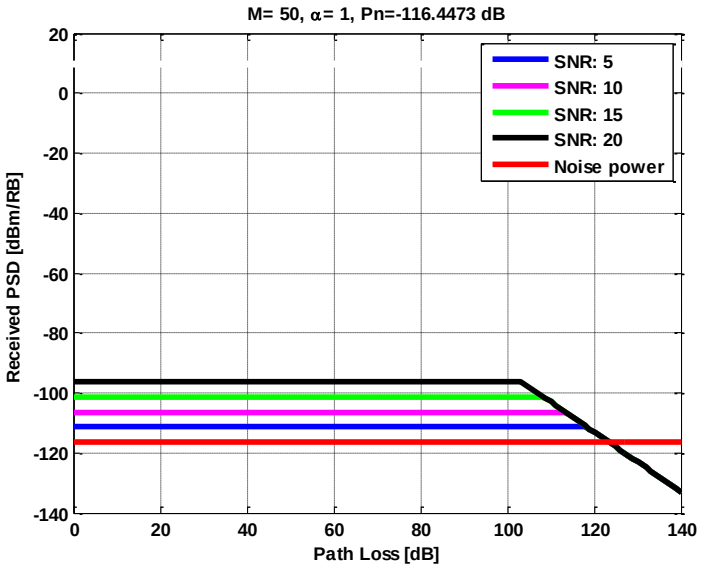

Figure 2-9: Plot of the received PSD for conventional power control scheme

The Figure 2-9 shows that the received PSD is same for all users independent of their path loss for given SNR target. It is worthwhile to note that the 'knee point' indicates the power limited region i.e. users at this point and beyond will start to use $P_{\max}$, in other words it shows the maximum path loss which results in uplink power equal to $P_{\max}$ by the user. The knee point drifts to the left by increasing the SNR target (SNR_0); this means that users will be power limited more quickly. High SNR_0 mostly favors users close to the eNB while lower SNR_0 favors users at the cell-edge.

2.4.4 Fractional power control scheme

The fractional power control scheme allows user to be received with variable PSD depending on their path loss i.e. the user with good radio conditions will be received with high PSD. Using $0 < \alpha < 1$, PSD is given by

$$PSD_{Tx} = P_0 + \alpha PL = \alpha \cdot (SNR_0 + Pn) + (1-\alpha)(P_{\max}) + \alpha PL \ \left[\text{dBm / PRB}\right] \quad (2\text{-}15)$$

In contrast to conventional power control which allows full compensation of path loss, fractional power control compensates for the fraction of the path loss, and this is the reason that it is named as fractional power control. The received PSD can be found by taking path loss in to account and is given by

$$PSD_{Rx} = P_0 + PL(\alpha - 1) \ \left[\text{dBm / PRB}\right] \quad (2\text{-}16)$$

Attention is drawn here by comparing eq. (2-14) and eq. (2-16), since received PSD in case of conventional power control scheme results in P_0 while in case of fractional power control scheme it also have an additional term $PL(\alpha - 1)$. As both P_0 and α are cell specific broadcasted towards the UEs by the eNB, meaning that they are same for all the

UEs, thus *PL* is the key factor in the eq. (2-16) that allows users to be received with different power spectral density. This behavior can be explained with the help of figure obtained using eq. (2-16).

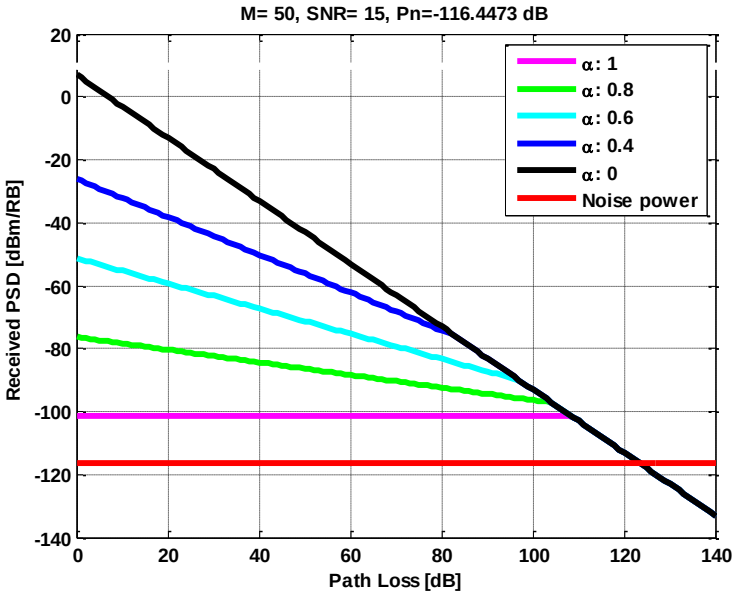

Figure 2-10: Plot of the received PSD for fractional power control scheme

In Figure 2-10, α = 1(full compensation) and α = 0 (no compensation) shows conventional and no power control scheme respectively, for 0 < α < 1 users are received with variable PSD depending on their path loss. The "knee point" drifts towards left by decreasing α and increasing SNR_0.

2.4.5 Open loop power control

Open loop power control is capability of the UE transmitter to set its uplink transmit power to a specified value suitable for receiver. This setting as discussed in section 2.4.2 is based on eq. (2-11), rewriting it as

$$P_{OL} = \min\{P_{\max}, 10 \cdot \log_{10} M + P_0 + \alpha \cdot PL\} \ [\text{dBm}] \qquad (2\text{-}17)$$

P_{OL} is the uplink power, set by open loop power control. The choice of α depends on whether conventional or fractional power control scheme is used. Using α = 1 leads to conventional open loop power control while 0 < α < 1 leads to fractional open loop power control.

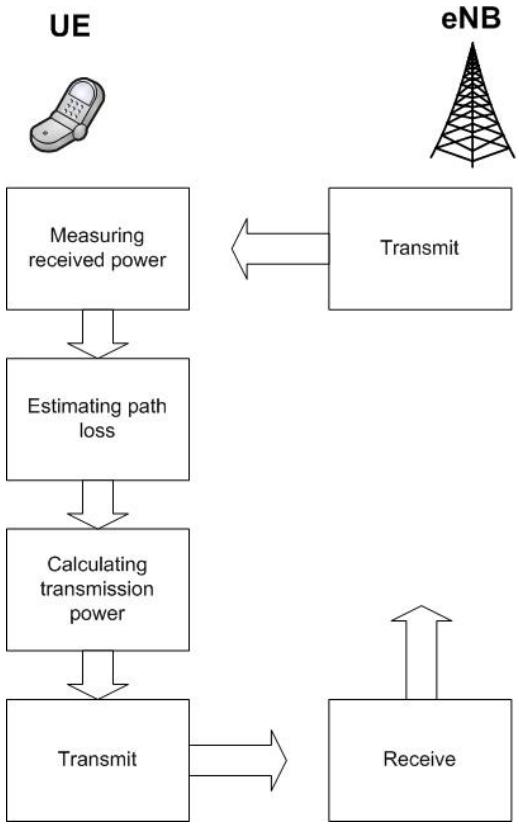

Figure 2-11 : Block diagram of steps involved in setting uplink power using open loop power control

The Figure 2-11 shows a block diagram of the steps involved in setting the uplink transmit power using the open loop power control. Estimate of the path loss is obtained after measuring reference symbol received power (RSRP) and then the calculation for transmission power is performed based on eq. (2-17). The transmit block in the eNB represents the broadcast of parameters involved in eq. (2-17), namely P_0 and α.

2.4.6 Closed loop power control

Closed loop power control is capability of the UE to adjust the uplink transmit power in accordance with the closed loop correction value also known as transmit power control (TPC) commands. TPC commands are transmitted, by the eNB towards the UE, based on the closed loop signal-to-interference and noise ratio (SINR) target and measured received SINR.

In a closed-loop power control system, the uplink receiver at the eNB estimates the SINR of the received signal, and compares it with the desired SINR target value. When the received SINR is below the SINR target, a TPC command is transmitted to the UE to request for an increase in the transmitter power. Otherwise, the TPC command will request for a decrease in transmitter power.

The LTE closed loop power control mechanism operates around open loop point of operation. As discussed in section 2.4.2, the UE adjusts its uplink transmission power based on the TPC commands it receives from the eNB when the uplink power setting is performed at the UE using open loop power control. The closed loop power control mechanism around open loop power of operation is presented in Figure 2-12.

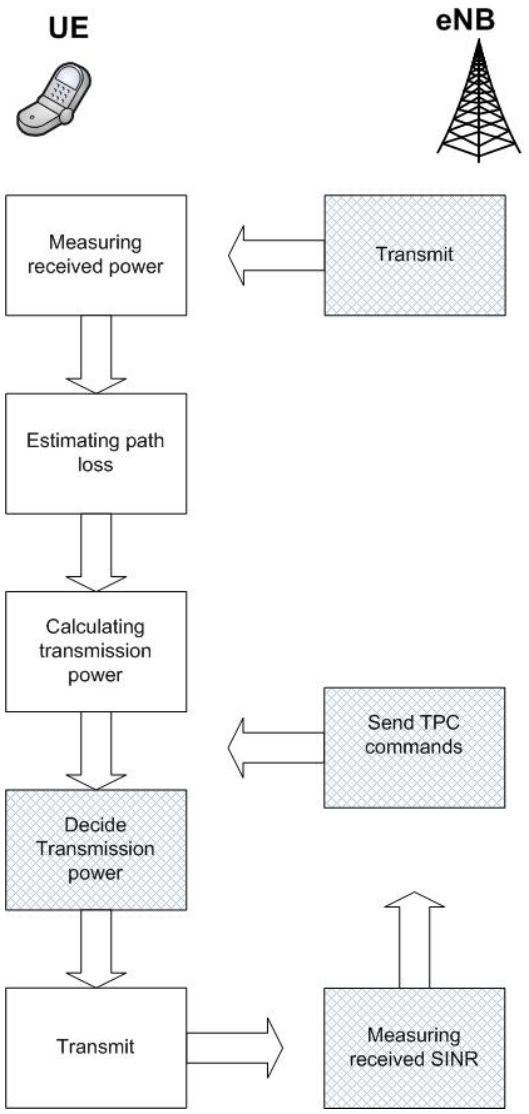

Figure 2-12: Block diagram of steps involved in adjusting open loop point of operation using closed loop power control.

The shaded blocks indicate the closed loop power control components. As shown in Figure 2-12, the closed loop correction value is applied after calculating the transmission power using the open loop power control.

It is worthwhile to note that, conventional and fractional power control indicates the choice of value of α, while open loop and closed loop power control indicates the method of setting the transmission power.

Chapter 3 Methodology

This chapter formulates the problem and provides a solution to overcome it. It also presents evaluation of path loss compensation factor for open loop, the implementation details of the conventional closed loop power control followed by a mathematical model of an implemented solution, and implementation details of the closed loop based on the proposed solution. Furthermore issues in the implementation of absolute error, SINR filtering, and time delay, including both the UE processing and round trip propagation time delays, are also discussed.

3.1 Problem formulation

To formulate the problem statement, uplink average received SINR is investigated for the conventional closed loop around open loop point of operation and the open loop power of operation only.

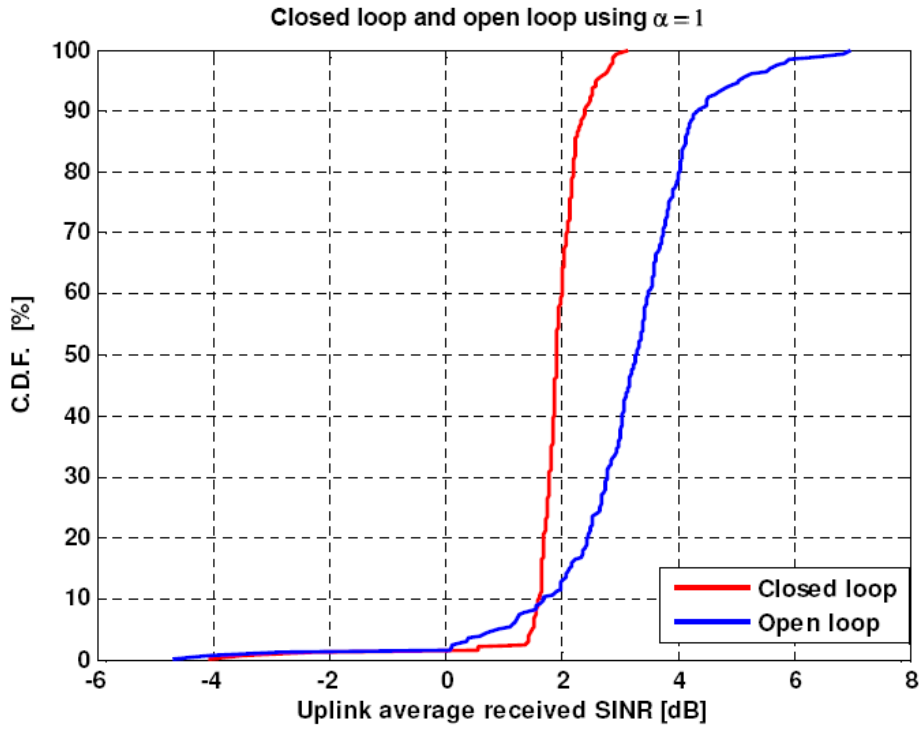

Figure 3-1: CDF plot of uplink average received SINR for open and closed loop power control using $\alpha = 1$

In Figure 3-1, the open loop power control allows users with good radio conditions (users close to the base station) to achieve high received SINR, resulting in high mean user bit rate while keeping reasonable cell-edge bit rate. In contrast to open loop, the

conventional closed loop steers all users to achieve equal received SINR, as a consequence of this, users with good radio conditions which can achieve high received SINR are affected, thus resulting in lower mean user bit rate. The users at the cell-edge are more affected by interference as compared to the users at the centre of the cell. In contrast to open loop power control, the closed loop power control compensates for interference, thus it provides better cell-edge user bit rate.

It is worthwhile to note that setting of the closed loop SINR target is a trade-off between the cell edge and mean bit rate i.e. high target results in high mean user bit rate but lower cell edge bit rate, while lower SINR target leads to low mean and high cell edge bit rate . Thus it is desired to design a closed loop power control scheme that can provide reasonable cell-edge bit rate and at the same time allowing users with good radio conditions to achieve high received SINR, thus providing high mean user bit rate.

3.2 Evaluation of fractional open loop power control

LTE PUSCH open loop PC with fractional path loss compensation factor has been evaluated using static simulations [3], which showed performance gain over conventional open loop power control in terms of cell edge and mean bit rate. However, in this thesis study, path loss compensation factor for the open loop power control is investigated using dynamic simulations.

The fractional open loop and its parameter setting are already discussed in [5]. However, some of the important aspects are discussed here for the sake of completeness. This discussion will also help in understanding the mathematical model of an implemented solution. As discussed in section 2.4.4, eq. (2-15) defines the power spectral density for the fractional open loop power control. The relation between the terms involves in eq. (2-15) is presented in the Figure 3-2.

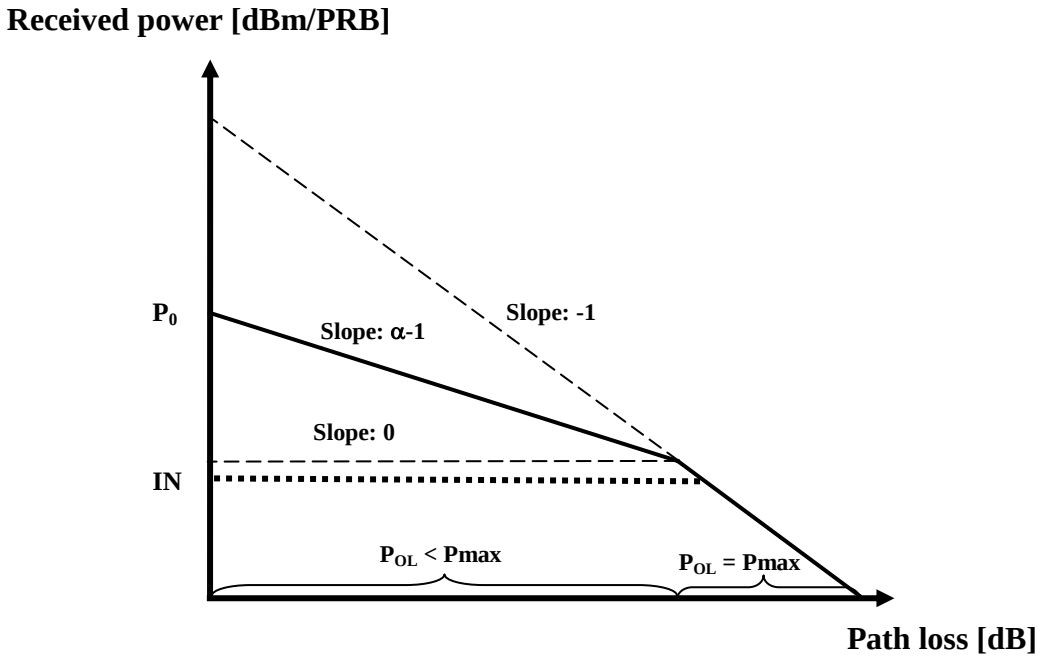

Figure 3-2: Relation of received PSD and path loss describing slopes for different power control algorithms

In section 2.4.2, power control schemes are categorized based on the path loss compensation factor. However, the slope of the received PSD is another way of categorizing different power control algorithms.

Figure 3-2 shows different slopes of the received PSD using different values for the $0 \leq \alpha \leq 1$. The slope results in α - 1 when $0 < \alpha < 1$, this leads to the fractional open loop power control, while using $\alpha = 0$ i.e. slope = -1, leads to no power control. Furthermore, using $\alpha = 1$ results in slope = 0 which leads to conventional open loop power control. The figure also defines the region where the users start using maximum allowed power; this is identified by the knee point. At the knee point and beyond, users will experience maximum path loss thus resulting in using maximum power.

The received PSD for fractional open loop power control is defined by eq. (2-16); it results in P_0 at zero dB path loss. The received PSD for the conventional and no power control schemes are shown using dashed line. For the conventional open loop power control, the received PSD is same for all the UEs independent of their path loss as shown in Figure 3-2.

3.3 Implementation details of conventional closed loop power control

LTE PUSCH closed loop power control operates around an open loop point of operation. The open loop power control is adjusted using closed loop correction value. eq. (3-1) defines the PUSCH closed loop power control expression.

$$P_{PUSCH} = \min\{P_{\max}, P_{OL} + f(\Delta_i)\} \quad [\text{dBm}] \tag{3-1}$$

P_{OL} is the uplink power set by the open loop point of operation and is calculated as $10 \cdot \log_{10} M + P_{0\_PUSCH} + \alpha \cdot PL$. The P_{OL} is also defined by eq. (2-17), here it is worthwhile to note that, if P_{PUSCH} is set using the closed loop power control then power limitation is neglected in eq. (2-17) and is applied by eq. (3-1). In case of the conventional closed loop power control, the open loop component uses $\alpha = 1$.

$f(\Delta_i)$ is the closed loop adjustment to open loop point of operation . It is defined [1] by the expression given below

$$f(i) = f(i-1) + \delta_{PUSCH}(i - K_{PUSCH}) \ [\text{dB}] \tag{3-2}$$

δ_{PUSCH} is UE specific correction value, also referred as TPC command. This study uses TPC commands [-1, 0, 1, 3] dB [1]. $f(*)$ represents accumulation while $f(0) = 0$ and K_{PUSCH} = 5 TTI. K_{PUSCH} includes both processing and round trip propagation time delay, this issue is discussed in section 3.7.1. The TPC commands are generated based on the difference between SINR target and received SINR, as shown in Figure 3-3.

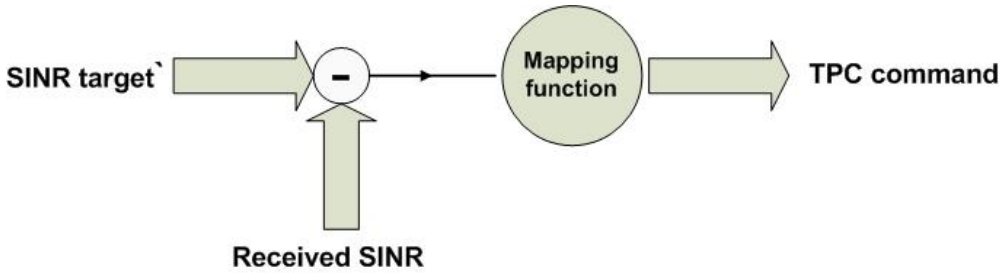

Figure 3-3: Generation of the TPC command at the eNB

The mapping function maps the resulting difference to one of the accumulate TPC commands. The generated TPC commands are transmitted by the eNB towards the UE. In this thesis study, the conventional closed loop SINR target used in the generation of TPC commands is referred to as baseline SINR target.

3.4 Implementation details of closed loop PC with fractional path loss compensation factor

Closed loop power control combined with fractional path loss compensation factor is implemented using eq. (3-1) which defines the basic expression for the closed loop power control, eq. (2-17) which is the open loop point of operation and eq. (3-2) defines the closed loop correction value. However, in contrast to conventional closed loop implementation which uses baseline SINR target and α = 1, closed loop with fractional

path loss compensation factor is implementation involves closed loop SINR target based on the path loss of the users and $0 < \alpha < 1$.

A mathematical expression that allows setting the SINR target based on the path loss of users is derived in section 3.4.2. Furthermore, investigation for finding optimal value for the path loss compensation factor that results in best cell edge and mean user bit rate is discussed in section 3.4.

3.4.1 Power headroom report

The power headroom report can be used by the eNB to calculate the path loss of the users which is then used in setting of SINR target. The setting of SINR target based on path loss of users is explained in section 3.4.2.

Power headroom report is sent by the UE to the eNB which indicates how much power UE is left with to start using full power. In other words, it is the difference between the UE transmit power and the maximum UE transmit power.

$$P_h = P_{\max} - P_{PUSCH} \ [\text{dBm}] \tag{3-3}$$

The following triggers [18] should apply to the power headroom reporting

- The path loss has changed by a threshold value, since the last power headroom report is sent. The threshold value can be [1, 3, 6, inf] dB.
- The time elapsed from previous power headroom report is more than Y transmission time intervals (TTIs). The parameter Y can take values [10, 20, 50, 200, 1000, inf] TTIs.

A power headroom report can only be sent when the UE has an UL grant. If one or several triggers are fulfilled when the UE does not have a grant the UE should send the report when it has a grant again.

3.4.2 Mathematical model for setting SINR target based on path loss of the users

A mathematical equation needs to be derived to set the closed loop SINR target based on the path loss of users while keeping the baseline SINR target for those users which are using full power i.e. $P_{\max}$. Therefore a relation is formed between received SINR and path loss of the users as shown in Figure 3-4.

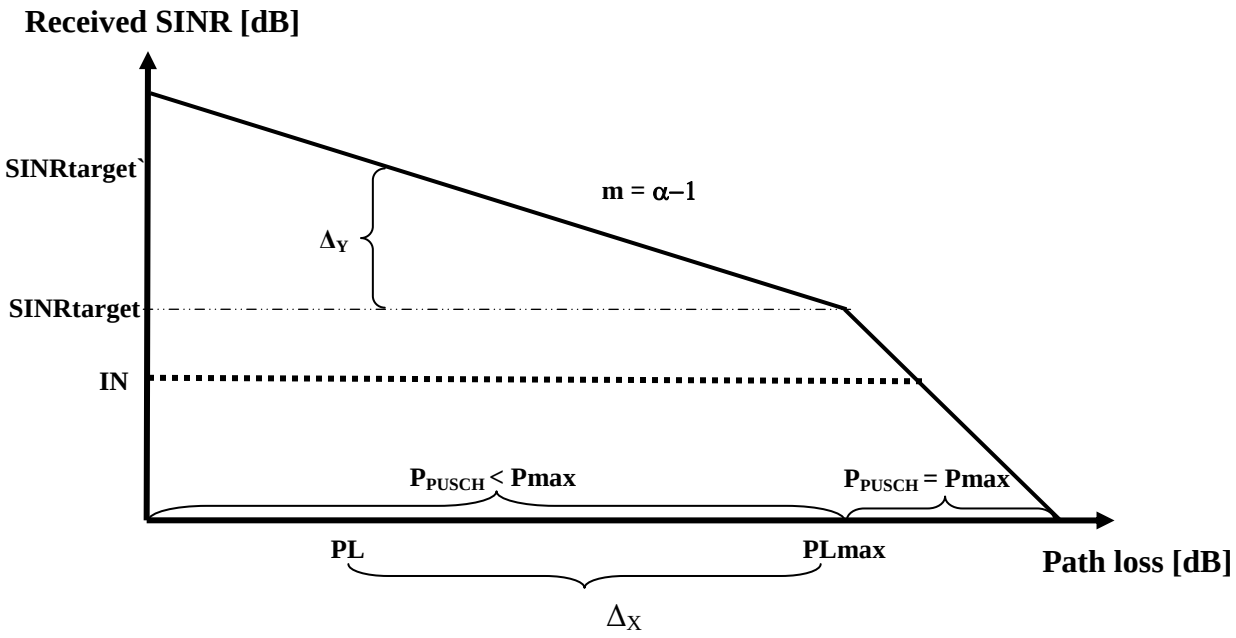

Figure 3-4: Illustration of setting SINR target based on the path loss of users

PL_{max} is the maximum path loss, at which users start using $P_{PUSCH} = P_{max}$. $PL < PL_{max}$ is path loss of any arbitrary user; SINRtarget is the closed loop baseline SINR target to start with. SINRtarget´ is the SINR target based on the path loss and α is the path loss compensation factor while m is the slope and is given by $\alpha - 1$, *IN* is the interference and noise power in dBm.

The knee point is denoted by PL_{max} i.e. users at this point and beyond will use P_{max}. Users at $PL < PL_{max}$ are at relatively good radio conditions than the users at $PL \geq PL_{max}$, therefore it is desirable that users should take advantage of their good radio conditions.

To derive a mathematical expression for setting of SINR target based on path loss of users; the information that is available at the eNB is the path loss (*PL*) of the users, baseline SINR target and PL_{max}. Thus the required mathematical equation that provides SINR target based on the path loss of users can be obtained using slope of the line and is given by

$$m = \frac{\Delta_Y}{\Delta_X} \tag{3-4}$$

where,

$$\Delta_Y = \text{SINRtarget}' - \text{SINRtarget} \ [\text{dB}] \tag{3-5}$$

$$\Delta_X = PL - PL_{max} \ [\text{dB}] \tag{3-6}$$

Using eq. (2-9), *PL* is given by

$$PL = \frac{1}{\alpha \cdot \{P_{PUSCH} - 10 \cdot \log_{10} M - P_0 - f(\Delta_i)\}} \ [\text{dB}] \qquad (3\text{-}7)$$

The path loss obtained using eq. (2-9) involves P_{PUSCH}, but in the real world, the eNB can use power headroom report (P_h) received by the eNB from the UE in order to find path loss of each user.

$$PL = \frac{1}{\alpha \cdot \{P_h - 10 \cdot \log_{10} M - P_0 - f(\Delta_i)\}} \ [\text{dB}] \qquad (3\text{-}8)$$

$P_h = P_{PUSCH} = P_{\max}$ when $PL = PL_{\max}$

It is worthwhile to note that calculation of PL using eq. (3-7) leads to ideal study of the closed loop power control with fractional path loss compensation factor. For realistic study PL is calculated using eq. (3-8), which involves power headroom reporting.

Using eq. (3-4) - (3-6) SINR target based on the path loss and is given by

$$\text{SINRtarget}' = \begin{cases} (\alpha - 1) \cdot (PL - PL_{\max}) + \text{SINRtarget} & , PL < PL_{\max} \\ \text{SINRtarget} & , PL \geq PL_{\max} \end{cases} \ [\text{dB}] \qquad (3\text{-}9)$$

In eq. (3-9), users at $PL \geq PL_{\max}$ will use SINRtarget´ = SINRtarget, indicating that there is no increase in the SINR target for users which are already using $P_{PUSCH} = P_{\max}$. Furthermore, $\alpha = 1$ turns the designed closed loop scheme into conventional closed loop power control meaning that the SINR target setting is independent of the path loss.

In case of the closed loop with fractional path loss compensation factor, TPC commands will be generated based on SINRtarget` and received SINR.

3.5 Investigating values for path loss compensation factor

In order to investigate different values for the path loss compensation factor, both the full buffer and simple upload traffic model are used. Full buffer and simple upload traffic models are discussed in detail in Appendix A. However, simple upload traffic model simulates more realistic behavior than the full buffer.

3.6 SINR filtering

Estimated received SINR is smoothened using an exponential filter. The general expression representing exponential filter is given below

$$Y(t) = (1 - \mu) \cdot Y(t-1) + \mu \cdot X(t) \ [\text{dB}] \qquad (3\text{-}10)$$

where

- $Y(t)$ is the output of the filter at time moment t.
- $Y(t\text{-}1)$ is the output of the filter at the previous time moment $(t\text{-}1)$.
- $X(t)$ is the input of the filter.
- $0 \leq \mu \leq 1$ is the filter parameter.

In simple words, the output $Y(t)$ of the exponential filter is the weighted sum of the previous output $Y(t\text{-}1)$ (taken with weight $1\text{-}\mu$) and the current input value $X(t)$ (taken with weight μ). The smaller the parameter μ, the longer the "memory" of the exponential filter and the greater the degree of smoothing the estimated received SINR.

The general expression is modified by introducing an additional factor; the modified expression is given by

$$Y(t) = (1 - \mu \cdot \frac{1}{m(t)}) \cdot Y(t-1) + \mu \cdot \frac{1}{m(t)} \cdot X(t) \ [\text{dB}] \quad (3\text{-}11)$$

where $m(t)$ is calculated as

$$m(t) = (1-\mu) \cdot m(t-1) + \mu \quad (3\text{-}12)$$

The factor $m(t)$ increases every time the user is scheduled, which means that the more frequent the user is scheduled the greater will be the value of $m(t)$ for this user. It means that the filter memory depends both on $m(t)$ and μ..

3.7 Delay and absolute error models

3.7.1 Processing and round trip time delay model

Time delay occurs between issues of a TPC command by the eNodeB but not yet received power adjusted transmission from the UE. This delay is typically propagation round trip time (RTT), processing time at the UE and the eNB. The total time delay used during simulations is of 5 ms. In detail explanation and demonstration of delay is discussed in Appendix B.

3.7.2 Absolute error model

The open loop power control error usually results from the factors such as accuracy of measurements of reference symbol received power (RSRP) at the UE and inaccuracies in the radio parts such as temperature sensitivity and tolerances in the standard. The absolute error is identified as a slowly varying component and varies between

manufactures of UEs. The sources of open loop power control error are shown in Figure 3-5.

At the time of writing, 3GPP had not yet standardized tolerance in the standard, but since the LTE RF components are the same as used in WCDMA, the tolerance described in the technical specification [9] can be used for first approximation. Tolerance of $\pm$ 9 dB is required, however a batch of UEs can handle $\pm$ 4 dB. Thus absolute error of $\pm$ 4dB with a uniform distribution is considered in order to evaluate the effect of the closed loop power correction using TPC commands. The eq. (3-13) defines the closed loop power control expression involving open loop error.

$$P_{PUSCH} = \min\{P_{\max}, P_{OL} + abserr + f(\Delta_i)\} \ [\text{dBm}] \tag{3-13}$$

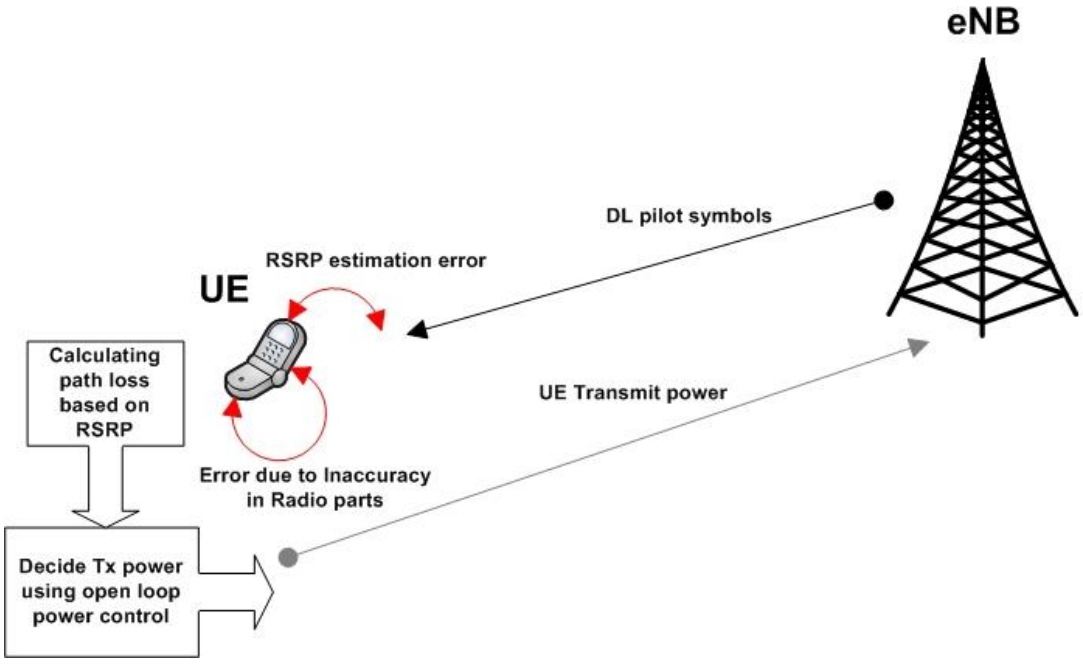

Figure 3-5: Illustration of the sources of open loop error including absolute error due to inaccuracy in radio parts

Chapter 4 Results and analysis

This section presents results obtained using both the full buffer and simple upload traffic models. As discussed in section 3.5, simple upload buffer model provides more realistic results and provides a better scale for performance analysis.

The results of performance comparison between open loop and closed loop power control with fractional path loss compensation factor are presented in Appendix C. Investigation for the optimal value of the PL compensation factor

4.1 Investigation for the optimal value of the PL compensation factor

Each value of α is investigated for each closed loop SINR target from a set of SINR targets. The criterion that selects optimal value of α for a given SINR target is optimized for cell-edge bit rate i.e. that value of α has been chosen which gives the best cell edge performance for a given SINR target.

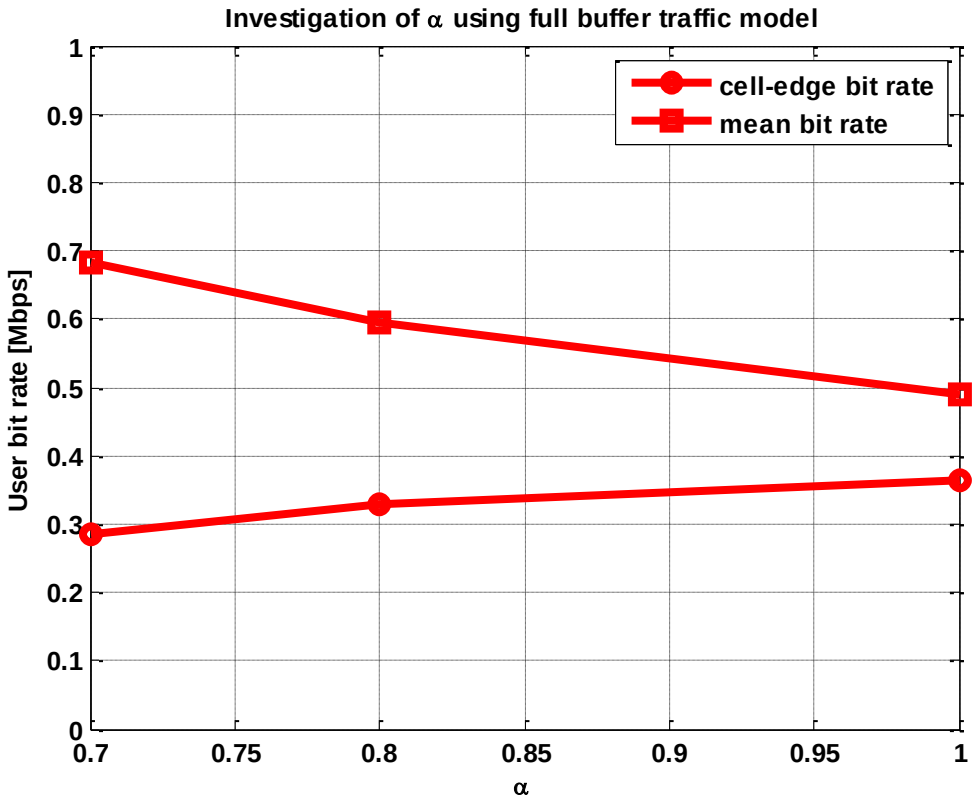

Figure 4-1: Investigating cell-edge and mean bit rate for different values of α for the closed loop power control using full buffer model.

The closed loop power control using α = 1 results in high cell-edge but relatively low mean bit rate as compared to other values of α, as shown in Figure 4-1. This behavior can be explained in a way that the system with α = 1 is less loaded in terms of bits as it is evident from the low mean bit rate, while using α = 0.8 and 0.7, user mean bit rate is relatively high meaning that users transmit more bits making the system more loaded. The increase in load may lead to rise the interference level and that's why the system using α = 0.8 and 0.7 have lower cell-edge bit rate when compared with α = 1.

It can be seen in Figure 4-1, the optimal value for α cannot be chosen using full buffer model as it leads to a trade-off between cell-edge and mean bit rate.

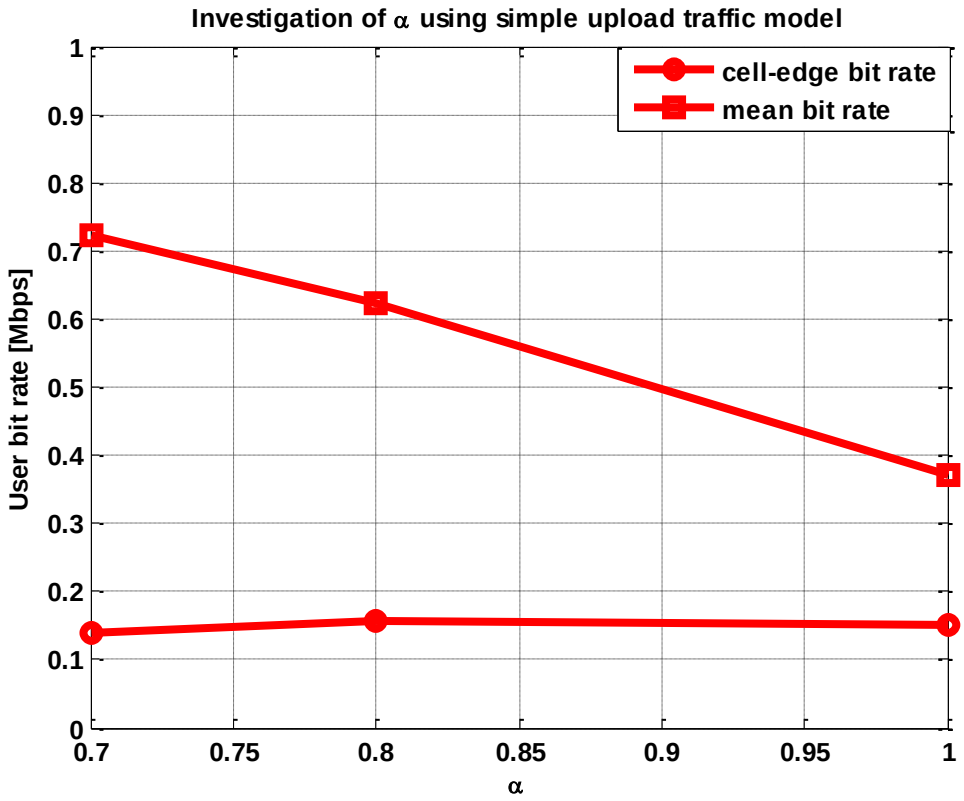

Figure 4-2: Investigating cell-edge and mean bit rate for different values of α for the closed loop power control using simple upload traffic model. The parameter settings are optimized for the best cell-edge bit rate

Using realistic traffic model in which user leaves upon transmitting the data, high mean bit rate is advantageous, because users can upload (transmit) their data more quickly than the system with low mean bit rate and thus can leave the system early.

In contrast to full buffer traffic model, α = 1 results in low cell-edge bit rate when compared to α = 0.8 using simple upload traffic model. This is because of the relatively high interference due to more users staying in the system for longer time. The users stay for longer time because they cannot transmit their data quickly due to the low mean bit rate, it is evident from Figure 4-2, the closed loop with full compensation resulting in

lower mean bit rate. The longer the users stay; the more will be the users in the system, which leads to high queuing delay and ultimately the interference will rise.

It is worthwhile to note that, at the end of simulation, the number of active users using $\alpha = 1$ were 2.6 % more than the active users using $\alpha = 0.8$; keeping in view that for each value of α the simulation started with equal number of users and lasted for equal amount of time. It shows that due to the high queuing delay using $\alpha = 1$, 2.6 % more users could not transmit all the data in their buffer.

Referring to the Figure 4-2, comparing $\alpha = 0.8$ and 1, it can be seen that $\alpha = 0.8$ results in high bit rate both in cell-edge and mean. The comparison of $\alpha = 0.7$ with $\alpha = 0.8$ and 1 leads to a trade-off between cell-edge and mean bit rate. Therefore 0.8 is a better value for fractional path loss compensation factor, as it results in best cell-edge and better mean bit rate.

4.2 Performance analysis of closed loop PC using $\alpha = 0.8$

The performance analysis of $\alpha = 0.8$ with the help of the CDF plots of the user bit rate and uplink received SINR is presented in the next figures. The performance evaluation is carried out both for the ideal and realistic cases. In the realistic study time delay, absolute error and power headroom reporting is taken into account, while in ideal case no delay, absolute error and power headroom is simulated.

4.2.1 Ideal case

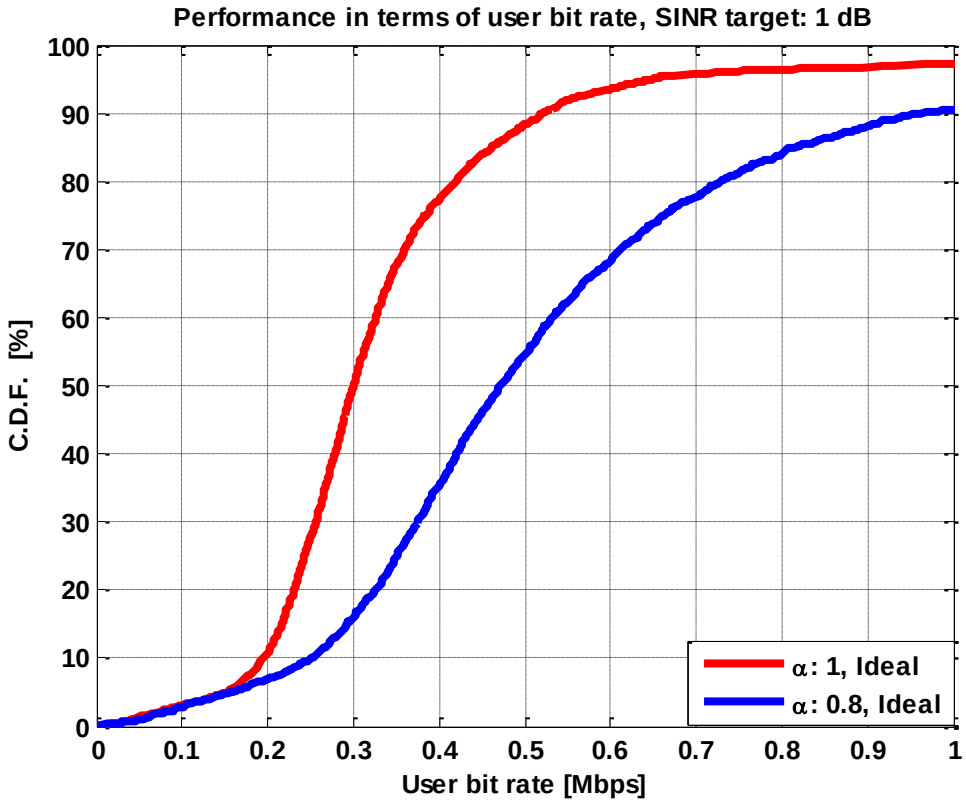

Figure 4-3: CDF plot of the user bit rate comparing α = 0.8 and 1.

As it can be seen in the Figure 4-3, the closed loop power control using α = 0.8 shows performance gain both in mean and cell-edge bit rate. The mean bit rate is improved by 68 % and at the same time providing better cell-edge performance than α = 1.

The next figure shows the performance comparison in terms of uplink average received SINR.

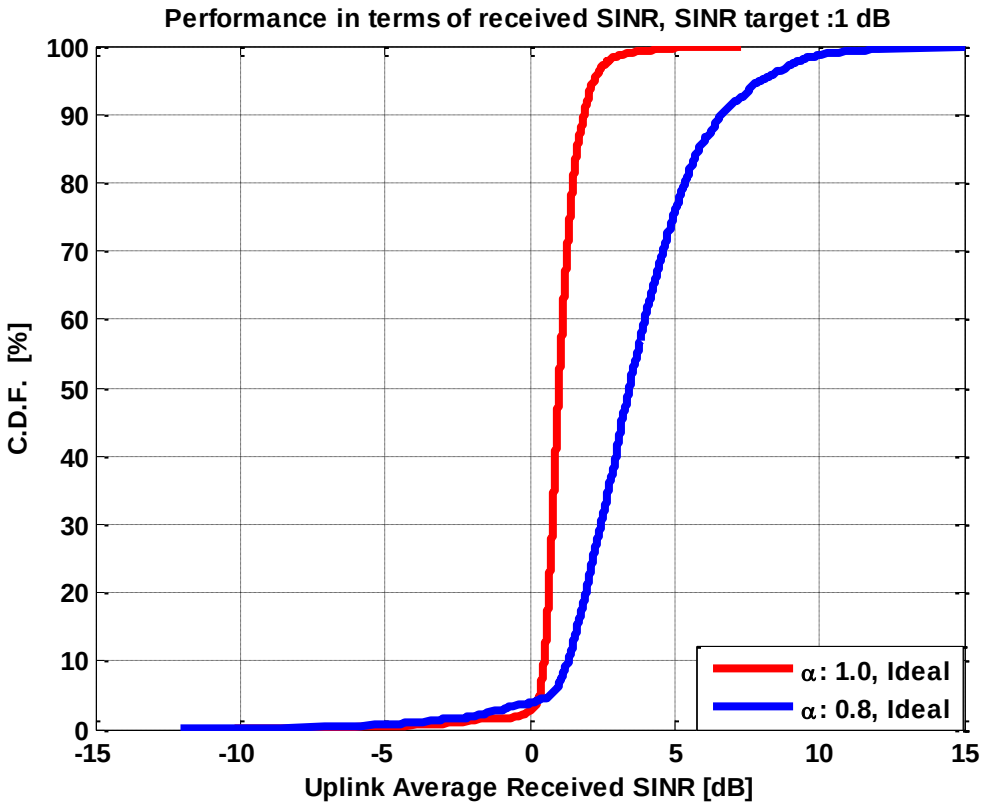

Figure 4-4: CDF plot of the uplink average received SINR using simple upload traffic model.

The closed loop power control with full compensation steers all users to achieve equal uplink average received SINR, as seen in Figure 4-4, both the 5th percentile users and the users close to the base station i.e. users with good radio conditions, all get equal received SINR because all the users aim to achieve same baseline SINR target.

In contrast to full compensation, the closed loop power control with fractional compensation keeps the baseline SINR target for the worst users and at the same time increases the baseline SINR target based for the users with good radio conditions based on their path loss, low path loss results in high increase in the SINR target.

The effect of SINR target setting based on path loss of the users is quite evident from the Figure 4-4, the better the radio conditions the higher is the average received SINR.

4.2.2 Performance analysis with absolute error and TPC delay

The effect of open loop error and TPC delay is analyzed in this section; both the individual and combined effect of open loop error and TPC delay is investigated.

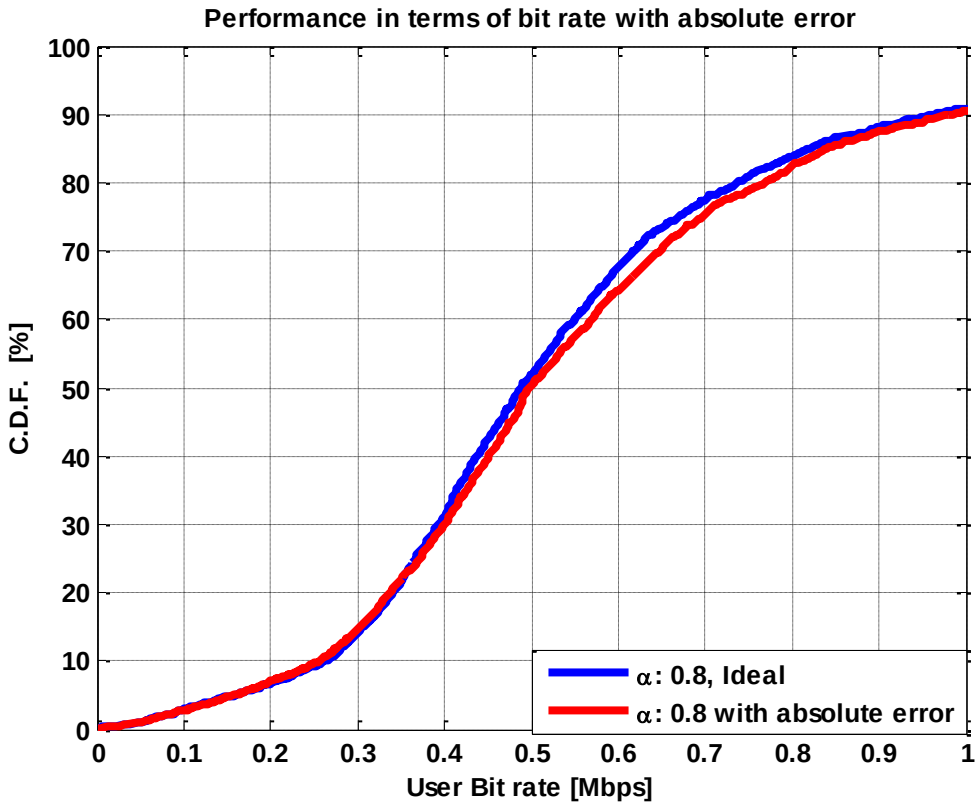

Figure 4-5: Performance of user bit rate when the absolute error is taken into account.

The performance of the user bit rate improved for the users with good radio conditions by taking open loop error in to account, it can be seen in Figure 4-5. This is because the uplink power increased due to open loop error for the number of UE resulting in high received SINR. The performance in terms of user bit rate slightly degrades for users in the low CDF region; this is because the number of UE cannot satisfy the required SINR due to open loop error. However, performance change in terms of bit rate due to absolute error is just the initial phenomenon and it will not be visible when simulated for longer time.

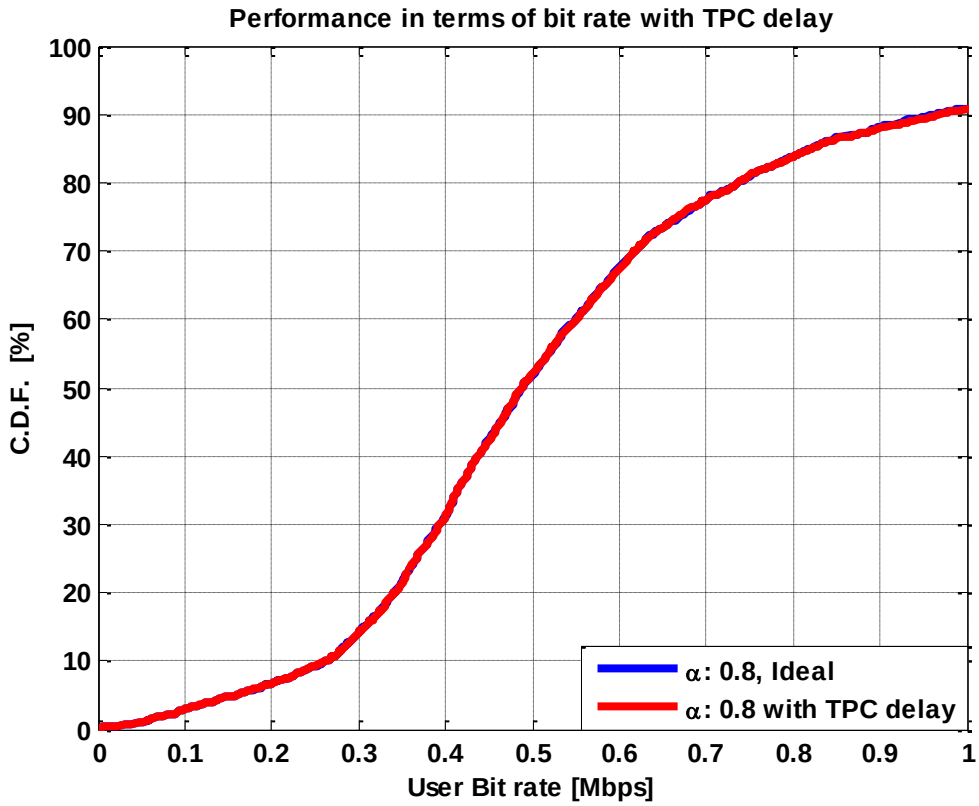

Figure 4-6: CDF plot of user bit rate showing both the closed loop power control with and without TPC delay. The total simulation time is 200ms.

The TPC delay introduces an initial delay of only 5 TTIs before the UE starts to use the TPC command it received from the eNB to correct its uplink power. It is worthwhile to note that, with the round robin scheduling it takes only 15 TTIs before all users start to correct their uplink power using the TPC command. Thus the effect of TPC delay is not visible, as can be seen in Figure 4-6, the closed loop power control with TPC delay shows same performance in terms of cell-edge and mean bit rate as that of the closed loop without TPC delay.

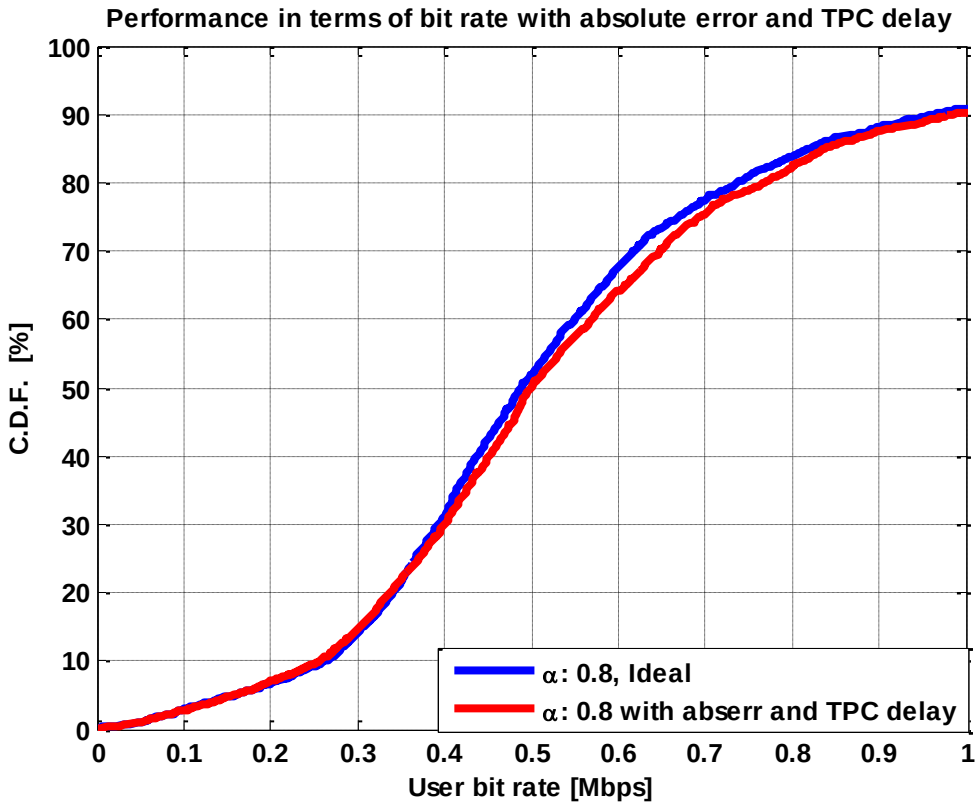

Figure 4-7: Performance in terms of bit rate with absolute error and TPC delay

The Figure 4-7 shows the combined effect of both the open loop error and TPC delay. However, as there is no noticeable effect of TPC delay as discussed above thus the effect on the user bit rate shown is due to the open loop error. Furthermore, Figure 4-7 is the same as Figure 4-5; the reason of this behavior due to open loop error is already discussed.

4.2.3 Performance analysis with power headroom report

In this section, the behavior of the closed loop power control with the power headroom reports is analyzed. The performance is analyzed using the power headroom triggers individually. Moreover, the combined effect of both the triggers applicable to the power headroom reporting is also analyzed.

4.2.3.1 Performance of power headroom report triggering at periodic intervals only

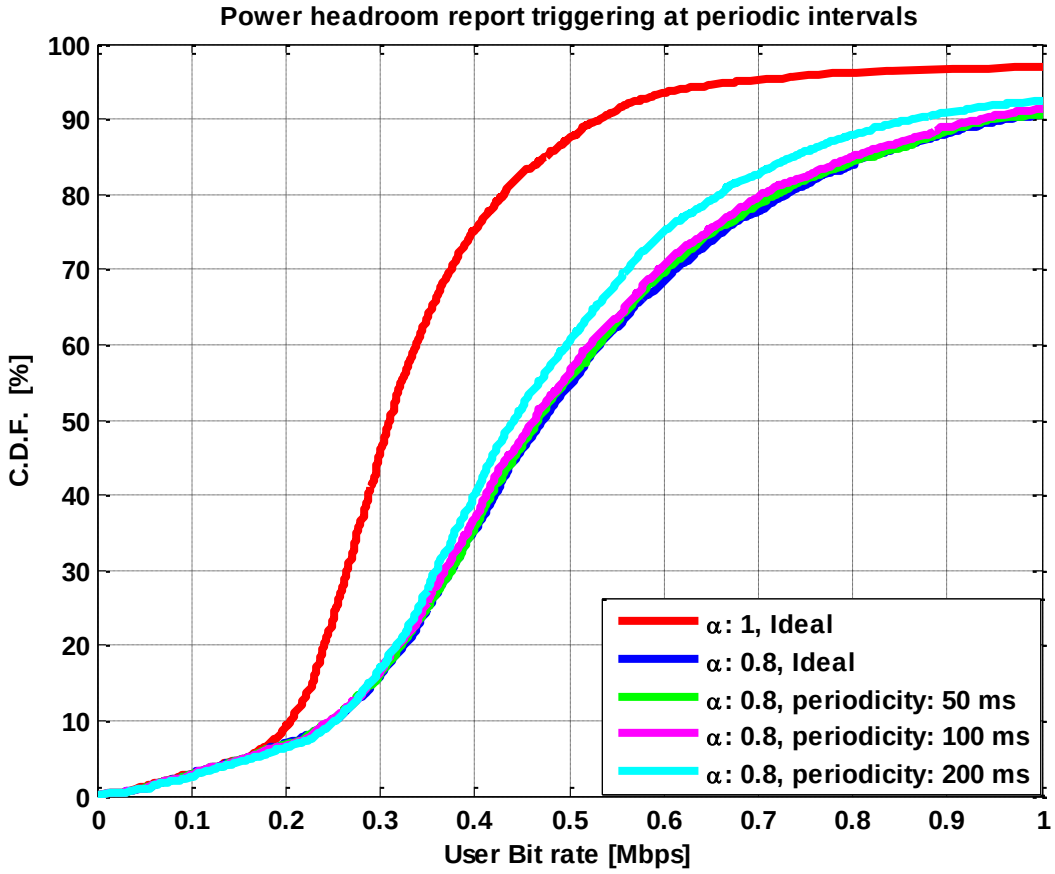

Figure 4-8: CDF plot of user bit rate. The power headroom report triggering after 50, 100 and 200 TTIs.

The performance comparison in terms of user bit rate of the closed loop power control with full compensation and the closed loop power control using $\alpha = 0.8$ with and without the power headroom report is shown in Figure 4-8. It can be seen that with the power headroom reports the user bit rate is degraded for the users with good radio conditions.

The reason of degradation in the mean bit rate is the SINR target setting based on outdated path loss. The SINR target setting based on the path loss aims to improve performance, in terms of bit rate, for the users with good radio conditions. Thus the more outdated the path loss the more will be the degradation in the mean bit rate, as can be seen in Figure 4-8 for high periodicity values.

It is worthwhile to note that, for a longer simulation time and setting the power headroom periodicity to infinity, the performance of the SINR target setting based on the path loss will be more like that of the absolute target setting.

4.2.3.2 Performance of power headroom report triggering at change in PL only

In order to analyze the behavior using the path loss change as the power headroom trigger; the mobiles speed is increased from 3 km/h to 120 km/hr and the path loss threshold is set to 1 dB, while the simulation time is kept the same. This is because that the mobiles speed of 3 km/h is too slow for the UEs to experience a change in the path loss by 3 dB.

It is worthwhile to note that the mobile speed is increased only for the sake of behavior analysis of power headroom trigger namely the path loss threshold. The mobile speed is 3 km/h in all other simulations unless otherwise stated.

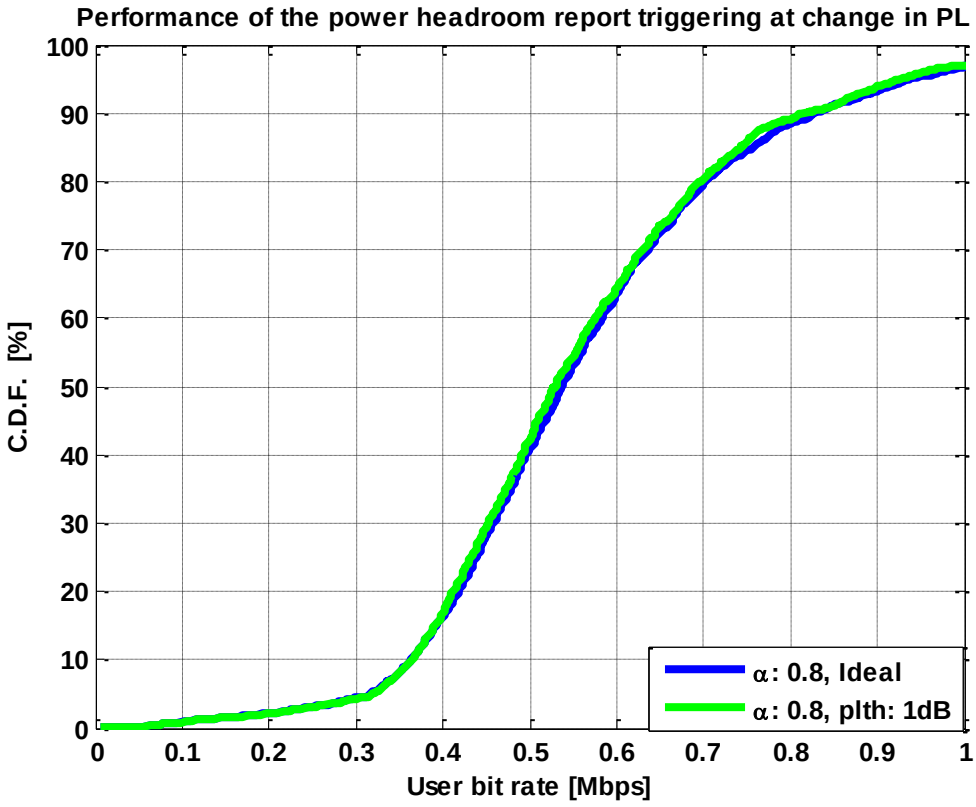

Figure 4-9 : CDF plot of bit rate showing the performance of power headroom report triggering at change in path loss. Full buffer traffic model, mobile speed of 120 km / h, and 1 dB path loss threshold is used. The simulation time is 200 ms

It can be seen in Figure 4-9, the mean bit rate is degraded slightly when power headroom report is used. This is because of the reason that eNB uses the outdated estimate of path loss until and unless the UE experiences the change in path loss greater than or equal to 1 dB. The degradation in performance will be more prominent by increasing path loss threshold value.

4.2.3.3 Performance comparison of the power headroom triggers

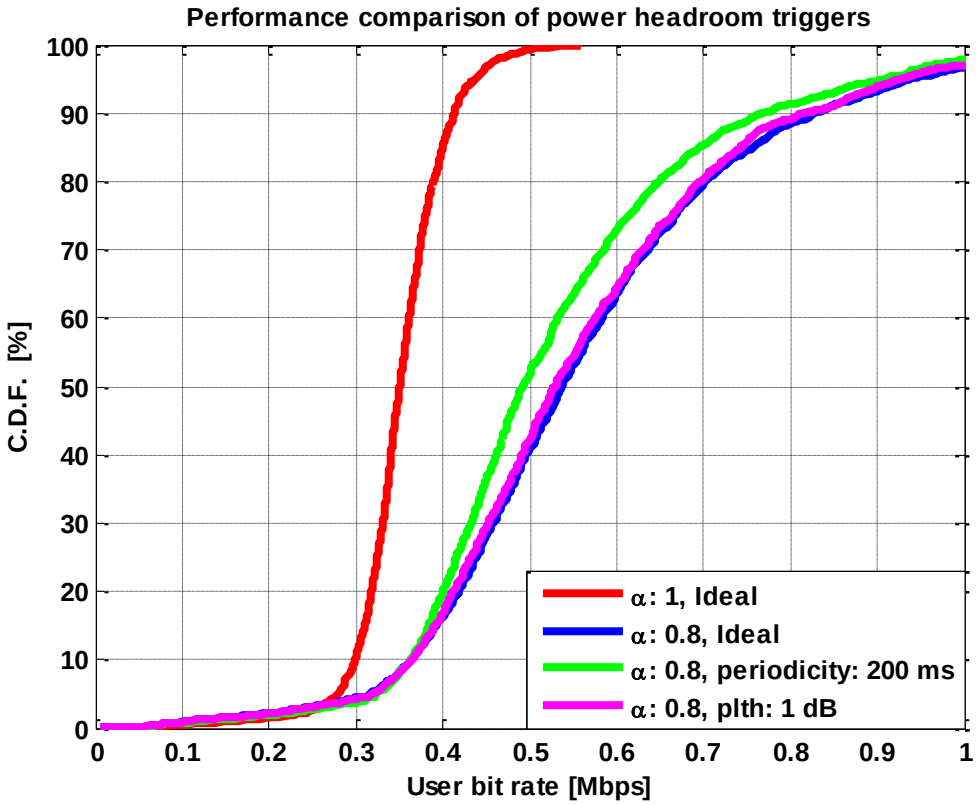

Figure 4-10: Performance comparison between the power headroom report triggering only at periodic interval and triggering only at change in the path loss.

The power headroom report triggering at the change in path loss results in better performance than triggering at periodic intervals, it can be seen in Figure 4-10, the mean bit rate is more degraded using the periodicity trigger than using the path loss threshold trigger.

The reason for more degradation using only periodicity as the power headroom trigger is that if any change in the UE uplink power occurs right after periodic interval then the UE have to wait for next interval to report the new uplink power. The longer the periodic interval the longer the UE has to wait to send the power headroom update thus the eNB will use more outdated estimate of the path loss.

On the other hand, triggering power headroom report when the path loss changes by a threshold value, the uplink power is reported immediately meaning that the eNB has more updated estimate of the UE path loss thus leading to better performance in terms of mean bit rate.

In this specific scenario, power headroom is reported only once using periodic intervals but on the other hand the power headroom was sent whenever the UE experienced the path loss change of 1 dB.

The next figure shows the performance comparison of using the path loss change alone as power headroom trigger and combination of both the triggers.

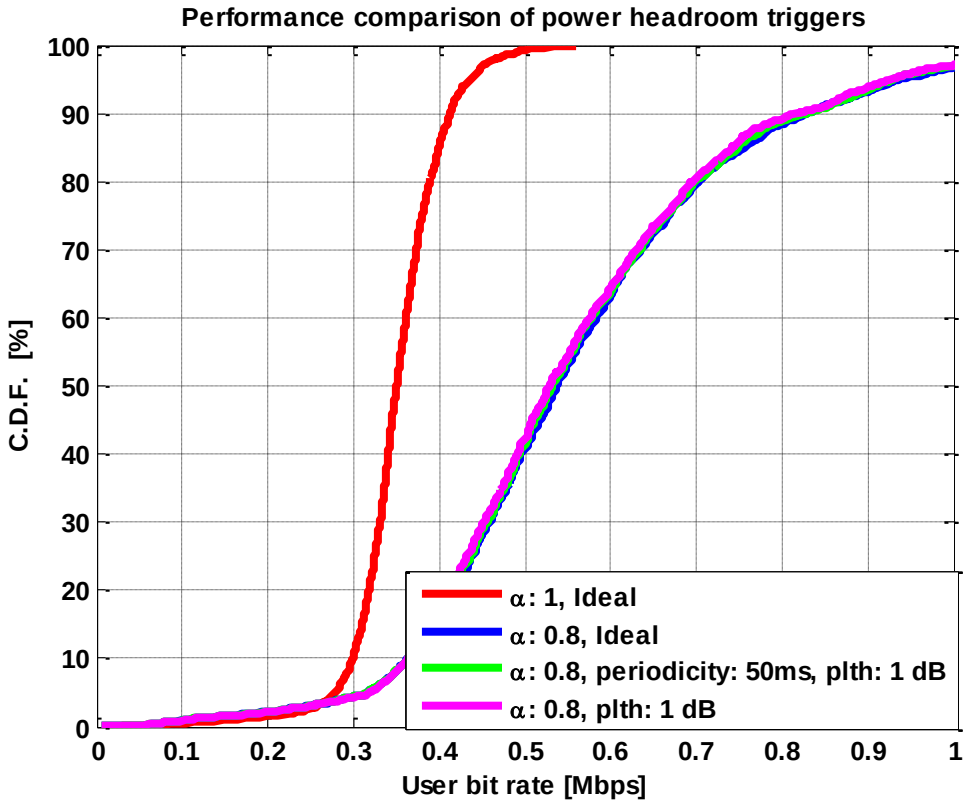

Figure 4-11: Performance comparison of the power headroom triggering at the periodic interval and change in path with the power headroom report triggering only at change in path loss

It can be seen in Figure 4-11, the performance of the power headroom report, triggering either at periodic intervals or when the UE experiences change in path loss is almost the same when use path loss change alone as a trigger to the power headroom report.

Comparing the power headroom report triggering at path loss change alone with the power headroom report triggering at periodic intervals or when the path loss changes by a threshold value of 1 dB, it is worthwhile to note that, in the latter case the uplink power is reported only four times more than in the former case, thus not making significant impact on the performance therefore resulting in same performance.

However, this shows that power headroom report triggering only at change in path loss results in less power headroom reporting overhead than using both the triggers.

4.2.4 Performance analysis with power headroom, TPC delay, and absolute error

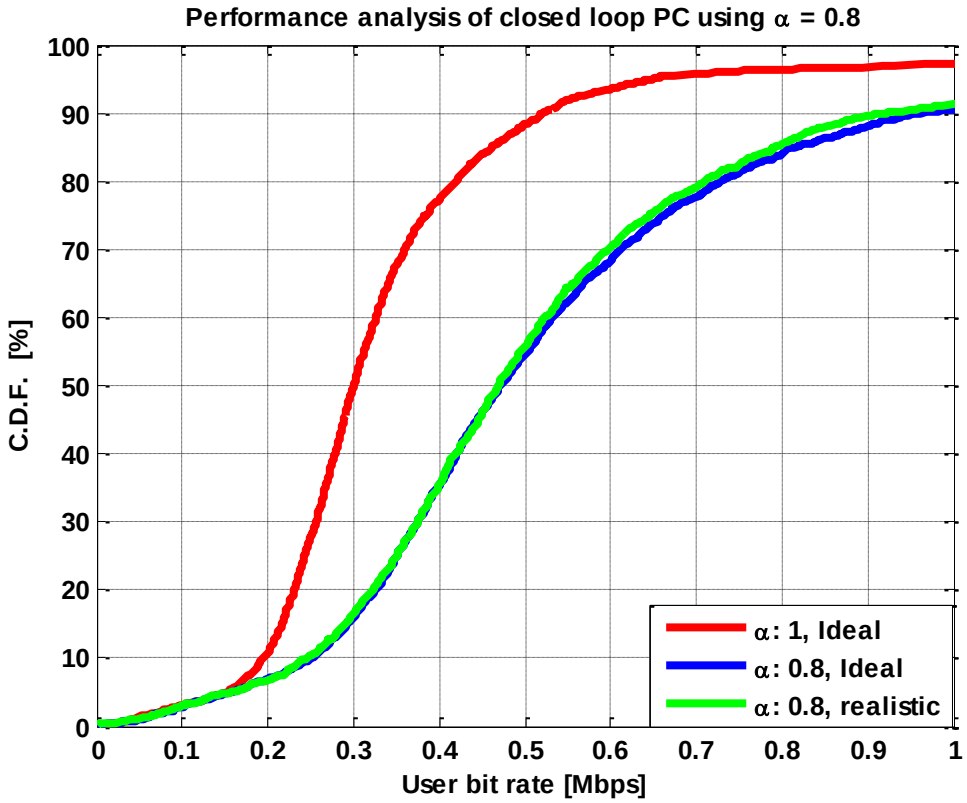

Figure 4-12 : Performance analysis in terms of user bit rate taking in to account power headroom report, absolute error, and time delay.

The performance in terms of user bit rate is analyzed taking into account the absolute error, time delay, power headroom report triggering at periodic intervals of 200 ms and when the path loss changed by a threshold value of 3 dB.

As it can be seen in the Figure 4-12, the closed loop power control using $\alpha = 0.8$ shows performance gain both in mean and cell-edge bit rate. The mean bit rate is improved by 63 % and at the same time providing better cell-edge performance than $\alpha = 1$.

4.2.5 Power utilization

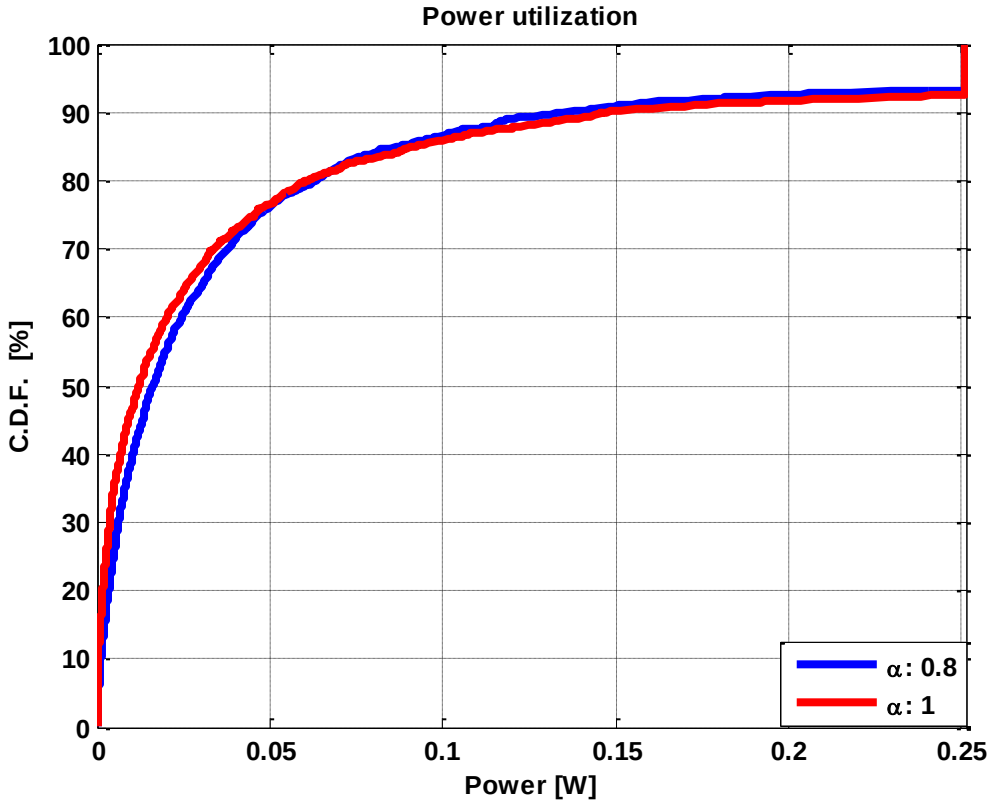

Figure 4-13: UEs power utilization using the closed loop power control with full and fractional compensation.

The difference of the mean of the UEs power consumption results in zero meaning that the overall power utilization is roughly the same using the closed loop power control with full and fractional compensation, as can be seen in Figure 4-13. However, the closed loop power control using $\alpha = 0.8$ utilizes battery power more efficiently as it provides better system performance in terms of cell edge and mean bit rate than the closed loop power control with full compensation.

Chapter 5 Conclusions & future work

This chapter summarizes and concludes the thesis work. It also presents the possible continuation of this work.

5.1 Conclusions

The LTE PUSCH closed loop power control with fractional path loss compensation factor was implemented using a dynamic radio network simulator. The performance evaluation was carried out using the full buffer and simple upload traffic model. Both the ideal and realistic cases were taken into account. In this thesis study, the realistic case included the performance evaluation by simulating the effect of absolute error of $\pm$ 4 dB, time delay, and power headroom report.

The path loss compensation factor was investigated for the values in the range 0.7 – 1. The closed loop power control with full compensation was used as a reference for performance comparison.

The simulation results indicated that conventional closed loop power control can be replaced by the closed loop power control with fractional compensation thus improving the system performance in terms of both the mean and cell-edge bit rate

In the ideal case, α = 0.8 showed performance gain over α = 1 by improving 68 % the mean bit rate at the same time providing the same cell-edge bit rate for a given SINR target.

The realistic results when compared with the ideal results showed that delay did not effect the performance of closed loop power control using α = 0.8. The absolute error showed performance gain in terms of mean bit rate because of the initial phenomenon of users arrived with high uplink power. However, the improvement due to initial phenomenon will not be prominent when simulated for longer time.

The performance of the closed loop power control using α = 0.8 was simulated with power headroom report triggering at periodic intervals or change in the path loss of the UE. It was found that with the use of power headroom report the performance was degraded in the mean bit rate due to the outdated path loss used in the setting of SINR target. Moreover, to study the impact on the performance when power headroom report is triggered at the change in path loss, the mobile speed was set to 120 km/h because the users were not experiencing path loss change of 1 dB at a speed of 3 km/h.

The performance comparison of both the triggers was also analyzed, the results showed that power headroom report triggering at change in path loss gives better performance than triggering at periodic intervals.

In the realistic case, the performance in terms of mean bit rate was improved by 63 % for a given SINR target. This shows that closed loop power control with fractional compensation is feasible to deploy without any significant degradation in performance.

5.2 Future work

This section presents few of the proposals that should be taken into account to improve the performance of closed loop power control with fractional path loss compensation factor. It also addresses couple of issues that demand attention to be investigated further.

The scheduling algorithm used was time division multiplexing (TDM); evaluation with different scheduling algorithms is an interesting enhancement.

LTE offers different modulation and coding schemes (MCS) and these should be included in further study. Furthermore, different antenna configuration can be used to analyze the performance behavior.

The error in the setting the uplink power control due to inaccuracy of UE's radio parts was taken into account in this thesis study; in order to make it more realistic an estimate of the error should be used rather than constant error value.

The error in estimation of path loss should also be taken into account for more realistic results.

In this thesis study, the filter performance with different parameter values is analyzed; it has been found that SINR filtering did not improve the performance of the power control scheme. It should be investigated further if performance can be improved by using a different scheduling scheme or changing some other parameters.

It was found that keeping SINR target constant and varying open loop SNR target makes a difference on final result. This is because of the convergence between SNR and SINR target. The more the difference between SNR and SINR target the more time it will take to converge. This should be investigated further in order to remove the impact of open loop SNR target on the performance of closed loop power control.

References

[1] 3GPP TS 36.213 V8.2.0 “E-UTRA Physical layer procedures”

[2] R1-074850 “Uplink Power Control for E-UTRA – Range and Representation of P0”

[3] R1-073036 “Intra-cell Uplink Power Control for E-UTRA – Evaluation of Fractional Path Loss Compensation**”**

[4] 3GPP, TR 25.814 v7.1.0. Physical layer aspects for Evolved UTRA

[5] Ericsson Internal “LTE uplink power control, overview and parameter setting”

[6] 3GPP TS 25.101 v8.3.0 User Equipment (UE) radio transmission and reception (FDD)

[7] 3GPP “3rd generation partnership project; Technical specification group radio access network; Spatial channel model for Multiple Input Multiple Output (MIMO) simulations”, 3GPP TR 25.996, V6.1.0

[8] J. Salo, P. Kyösti, and G. del Gado ”Implementation Specification of SCM model”, IST-2003-507581, 2004-09-30

[9] D. Baum et.al. ”An Interim Channel Model for 4G Systems, Extending the 3GPP Spatial Channel Model (SCM)” in *proceedings of IEEE Vehicular Technology Conference 2005 Spring (VTC’05-Spring)*, May 2005

[10] IST-2003-507581, WINNER Deliverable D5.3 “Interim Report on Link Level and System Level Channel Models”, version 2.50

[11] IST-2003-507581, WINNER Deliverable D5.4 “Final report on Link Level and System Level Channel Models”

[12] G. L. Stuber. Principles of Mobile Communication. Kluwer Academic Publisher, Boston, MA, USA, 1996

[13] W. C. Jakes. Microwave mobile communications. John Wiley & Sons, New York, NY, USA, 1974.

[14] M. Hata. Empirical formula for propagation loss in land mobile radio services. IEEE Transactions on Vehicular Technology, 29(3), 1980.

[15] Y. Okumura, E. Ohmori, T. Kawano, and K. Fukuda. Field strength and its variability in VHF and UHF land-mobile radio service. Review of the Electrical Communication Laboratory, 16(9-10), 1968.

[16] J. H. Winters, “Optimum Combining in Digital Mobile Radio with Co-channel Interference”, in IEEE Journal on Selected Areas in Communications, Vol. SAC-2, No. 4, July 1984.

[17] J. C. MAXWELL, A dynamical theory of the electromagnetic field, Royal Society Transactions,155 (1864)

[18] R4-081162 “LS on power headroom reporting”

[19] Simonsson, Arne Furuskar, Anders “Uplink Power Control in LTE - Overview and Performance, Subtitle: Principles and Benefits of Utilizing rather than Compensating for SINR Variations” Vehicular Technology Conference, 2008. VTC 2008-Fall. IEEE 68th

Appendix A Simulator details

This appendix describes the most relevant aspects of the system model. It also summarizes the default simulation parameters used for the simulations in this thesis study.

A.1 Path loss and channel models

The distance attenuation between two nodes is determined using 'standard' radio propagation models with the path loss (L) as a function of the distance *d*, on the form as defined by eq. (A- 1) below, and shadow fading is modeled as a log-normally distributed random variable.

$$L(d) = \beta + 10 \cdot \alpha \cdot \log_{10}(d) \quad [\text{dB}] \tag{A- 1}$$

The implemented channel model is based on the 3GPP spatial channel model (SCM) [7], which is a ray-based channel model that captures spatial and temporal channel characteristics.

A.2 Link quality model

The simulator uses a link quality model to estimate the probability that a channel coded block is erroneously decoded at the receiver side (after transmission over a multi-state channel). This error probability is often called the block error probability (BLEP). The used link quality model may be referred to as a two-step procedure. In the first step, the SINRs of the symbols in the channel coded block are calculated. In the second step, the BLEP of the code-block is estimated using a mutual information-based mapping function. A random experiment finally determines whether the block could be decoded successfully or if an error occurred.

A.3 SINR calculations

The SINR after receiver processing is calculated and used for BLEP estimation. The SINR depends on the used transmit weights, the channel and the interference as experienced at the receiver side. Two receiver antenna combining schemes are supported, namely maximum ratio combining (MRC) and interference rejection combining (IRC). In this thesis study IRC is used.

A.4 BLEP estimation

Once the SINRs of the symbols in the channel code block have been calculated, a mutual-information based link-quality model is used to estimate the block error probability. Given the symbol SINRs and the used modulation scheme, the mutual information (for bit interleaved coded modulation) carried by the symbol is calculated. The total, or the

average, mutual information over the code block is then mapped to the corresponding block error probability. The mapping of average mutual information to BLEP depends on the type of channel code used and the channel code rate.

A.5 Traffic models

The simulator supports variety of traffic models, however, two of the traffic models are used in this thesis study namely full buffer and simple upload traffic models. The traffic models are based on Poisson processes for user arrivals. Different arrival intensities may be given for different services.

Full buffer traffic model

In full buffer model, neither a user leaves due to hang up, nor does a new user arrive, because each user buffer is filled with infinite data and the user will not leave until and unless it transmits all the data. Thus the users remain the same in the entire simulation. This kind of buffer model does not reflect the realistic scenario; however, it is used for performance comparison of different power control schemes.

Simple upload traffic model

The simple upload traffic model is designed in a way such that the users can have limited data in their buffers, thus a user leaves when it transmits the data and new users is added in the system. It provides the ease to define the user upload file size, mean bearer bit rate. The mean bearer bit rate along with the offered cell throughput defines the total number of users in the system.

Moreover, simple upload buffer model allows calculating user bit rate involving the effect of queuing delay. The queuing delay reflects more realistic results and provides a better scale for performance comparison in choosing optimal value of α. For different values of α, the 5^{th} percentile and mean user throughput is calculated involving the effect of queuing delay. The queuing delay reflects more realistic results and provides a better scale for performance comparison in choosing optimal value of α. The calculation of bit rate involving queuing delay is discussed in 0.

The level of interference varies in both the traffic models. However, the interferers are the same in the entire simulation in case of full buffer model as opposed to simple upload traffic model, because users neither leave nor arrive in full buffer traffic model. This kind of buffer model does not reflect the realistic scenario. This is one of the reasons that the full buffer does not reflect realistic scenario, and thus this thesis study mostly focused on the results obtained using simple upload traffic model.

A.6 Noise model

Thermal noise has been modeled which has a constant power spectral density over a physical resource block. Its level is −116.4473 dBm/Hz, which doesn’t vary in time

A.7 Default simulation parameters

The default system simulation parameters are shown in Table A1.

Traffic models	
User distribution	Uniform
User mobile	3 km/h
Data generation	Full buffer, Simple upload traffic model
Radio network model	
Distance attenuation	L = 35.3+37.6*log(d), d = distance in meters
Shadow fading	Log-normal, 8dB standard deviation
Multipath fading	SCM, Suburban macro
Cell layout	Hexagonal grid, 3-sector sites, 21 sectors in total
Cell radius	167m (500m inter-site distance)
System models	
Spectrum allocation	10MHz (50 resource blocks) 180kHz (1 resource block)
Max UE output power	250mW into antenna
Max antenna gain	15dBi
Modulation and coding schemes	QPSK and 16QAM, turbo coding
Scheduling algorithm	Round robin
Receiver	MMSE [16] with 2-branch receive diversity

Table A 1: Default simulation parameters

Appendix B Time delay and bit rate calculation

B.1 Processing and round trip time delay

The time delay discussed in section 3.7.1 is demonstrated with the help of figure given below.

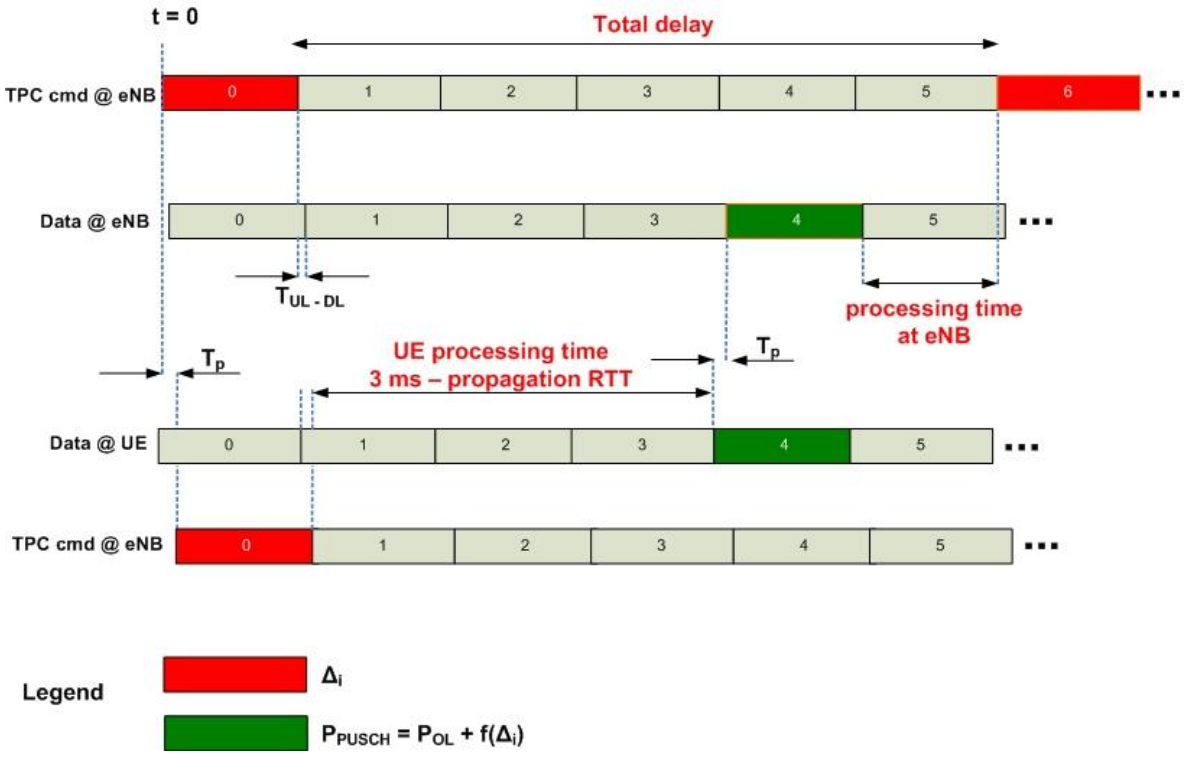

Figure B- 1: Illustration of time delay

In the Figure B- 1, T_{UL} - T_{DL} is the difference between duration of UL and DL subframe. T_p is the propagation time; round trip propagation time is 2 x T_p. It is assumed that the eNB received first transmission from the UE; the TPC command is generated based on the difference between SINR target and the received SINR measured at the eNB.

At the time instant t = 0, the eNB sent TPC command and received by the UE after the delay equal to half of the propagation RTT i.e. T_p. The processing time at the UE is 3 ms – propagation RTT[6], thus the UE have to adjust the power and transmit half of the propagation time before t = 4. The power adjusted transmission is received by the eNB at t = 4 and decoded at t = 5. Thus total time delay is 5 ms as shown in Figure B- 1.

As a consequence of 5 time instant delays, the eNB must take into account previous TPC commands while issuing new TPC command. Let say, the UE power needs to be adjusted by a single TPC command of +1dB and is issued by the eNB at time instant t= 0. Now until time instant t = 6, the eNB will receive transmission without closed loop adjustment,

if the eNB continues issuing TPC commands independent of previously issued TPC commands then UE will end up at +5 dB more increase in P_{PUSCH}.

To prevent this phenomenon sum of previously issued TPC commands are fed back to the mapping function, as illustrated in Figure B- 2. Thus new TPC commands will be generated based on SINR target, estimated received SINR and previously issued TPC commands.

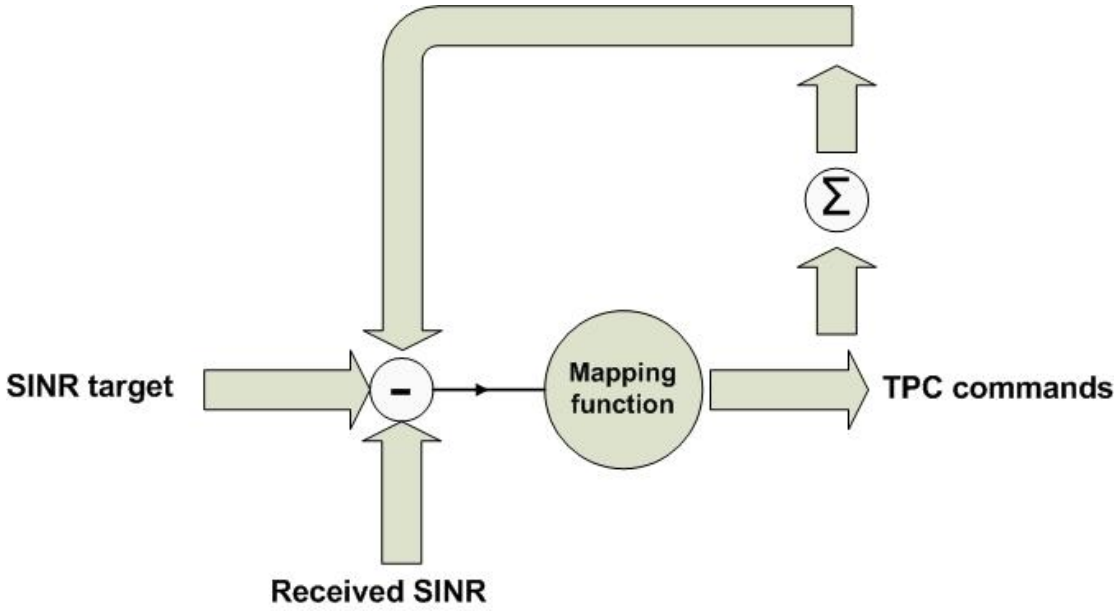

Figure B- 2: Generation of TPC commands at eNB taking into account previously issued TPC commands

Now as previously issued commands are taken into account by the eNB then in between t = 1 and t = 6, TPC command of 0 dB will be transmitted towards UE.

B.2 Bit rate calculation

In this thesis study, radio link and user bit rate is used to analyze the behavior of the power control schemes. The method of calculating radio link and user bit rate is different. This section describes the basic difference between these two methods of calculating the bit rate.

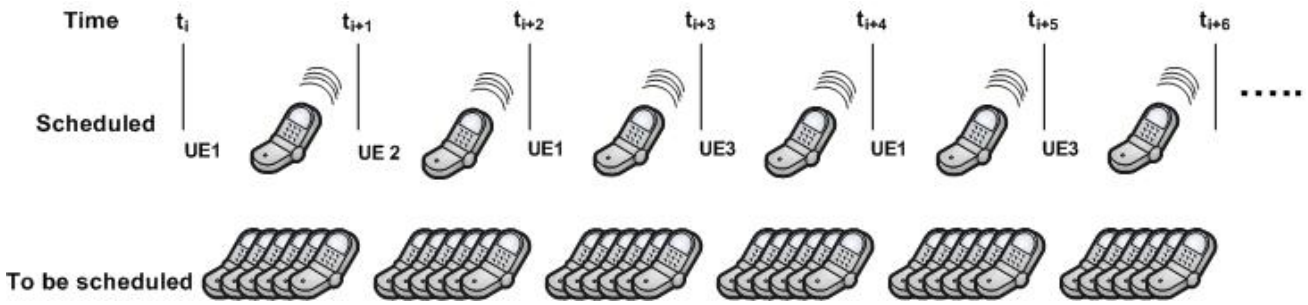

Figure B- 3: Illustration of radio link bit rate, it is assumed that the scheduling scheme is round robin

It can be seen in Figure B- 3, a number of UEs are waiting to be scheduled in order to transmit their data. Each UE, when scheduled, transmits for a certain time e.g. UE1 successfully transmit its data by making 3 transmission, thus the radio link bit rate for UE1 can be calculated using eq. (B- 1)

$$Radio\ link\ bit\ rate = \frac{Number\ of\ transmitted\ sucessfully\ bits}{Number\ of\ transmission\ attempts \times time\ unit}\ [\text{bps}] \qquad \text{(B- 1)}$$

In order to calculate the perceived bit rate by UE1, the queuing delay should be taken into account. The queuing delay refers to the amount of time a UE waits to be scheduled. For example UE1 starts transmitting data at t_i and let say it ends up transmitting the data at t_{i+5}, then the user bit rate can be calculated as

$$User\ bit\ rate = \frac{Number\ of\ transmitted\ sucessfully\ bits}{(End\ time - Start\ time)}\ [\text{bps}] \qquad \text{(B- 2)}$$

The *Start time* is the time when users is scheduled for the first time to transmit data while the *End time* represents the time at which the user ends up to transmit the data. It is worthwhile to note that is always less than or equal to radio link bit rate.

Appendix C Open loop power control results

This section presents the performance comparison of the closed loop and open loop power control for different values of the path loss compensation factor. Furthermore, the performance of open loop in the presence of the UE's absolute error is also discussed.

C.1 Performance comparison for different values of the PL compensation factor

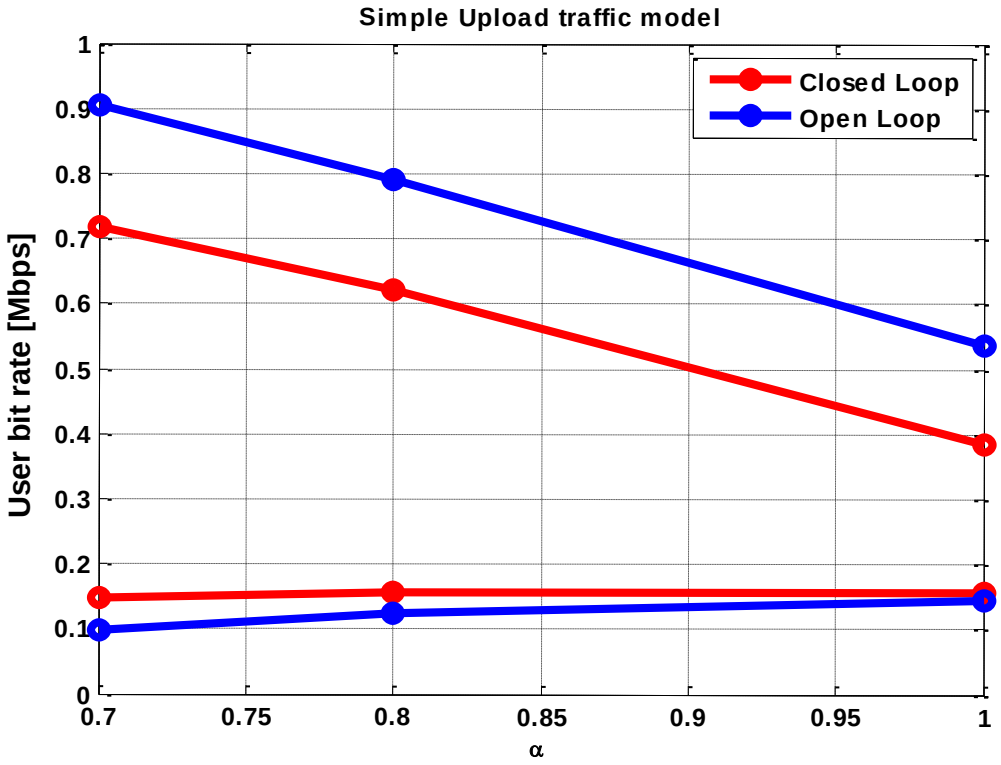

Figure C- 1: Open loop versus closed loop, the plotted values are optimized for best cell-edge bit rate

It can be seen in Figure C- 1, the closed loop power control using α = 0.8 shows performance gain, in terms of cell-edge and mean bit rate, over open loop power control with full compensation.

However, comparing closed loop and open loop power control for same value of α = 0.8, it leads to a trade-off between cell-edge and mean user bit rate.

C.2 Effect on the performance due to absolute error

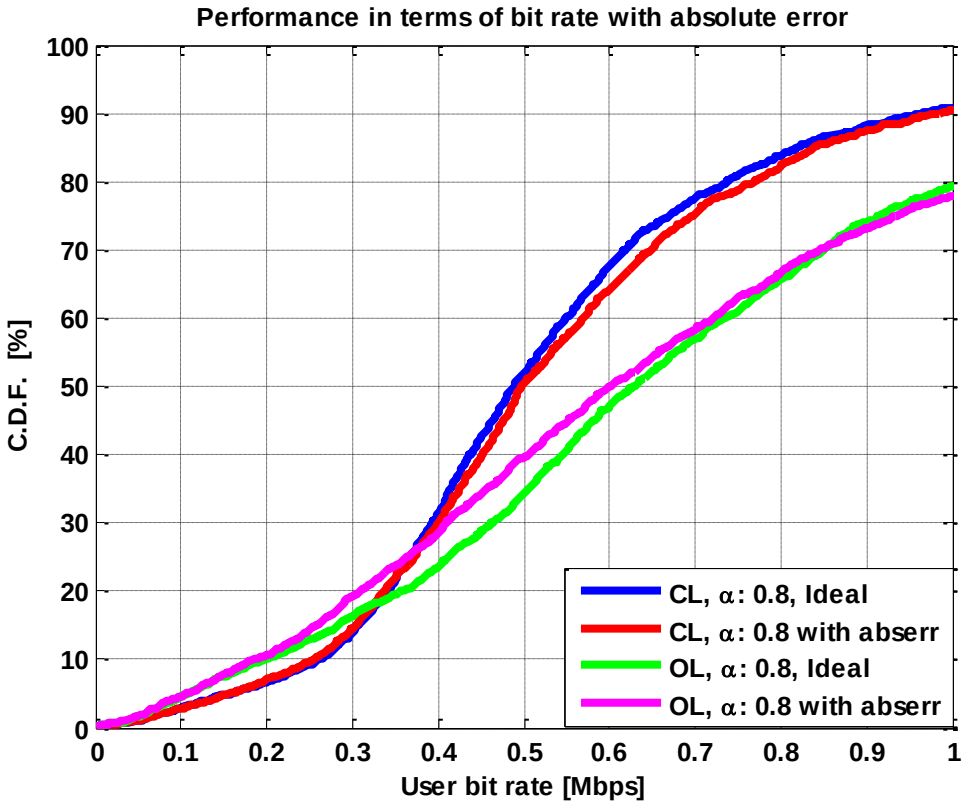

Figure C- 2: Performance comparison, in terms of bit rate, between closed loop and open loop power control in the presence of absolute error

The open loop performance is degraded, both in the cell-edge and mean bit rate, in the presence of absolute error, as can be seen in Figure C- 2. In contrast to open loop, there is no significant performance degradation in the cell-edge bit rate using closed loop power control. The slight degradation in the cell-edge is due to the users not satisfying the required SINR; the significant improvement in the mean bit rate is due to the users arriving with high power thus achieving high SINR.

However, using closed loop power control, this change in performance due to absolute error would not be noticeable in longer simulation, because it takes time to adjust the power of the UEs using TPC commands. In contrast to closed loop power control, there is no compensation of the absolute error in open loop power control, thus the open loop power control is susceptible to performance degradation in the presence of absolute error.